JOURNAL OF VIROLOGY, Dec. 2008, p. 11651–11668 Vol. 82, No. 23
0022-538X/08/$08.00+0 doi:10.1128/JVI.01762-08

Profiling the Specificity of Neutralizing Antibodies in a Large Panel of Plasmas from Patients Chronically Infected with Human Immunodeficiency Virus Type 1 Subtypes B and C▽†

James M. Binley,[1] Elizabeth A. Lybarger,[2] Emma T. Crooks,[1] Michael S. Seaman,[3] Elin Gray,[4] Katie L. Davis,[5] Julie M. Decker,[5] Diane Wycuff,[2] Linda Harris,[6] Natalie Hawkins,[6] Blake Wood,[6] Cory Nathe,[6] Douglas Richman,[7] Georgia D. Tomaras,[8] Frederic Bibollet-Ruche,[5] James E. Robinson,[9] Lynn Morris,[4] George M. Shaw,[5] David C. Montefiori,[8] and John R. Mascola[2]*

Torrey Pines Institute for Molecular Studies, 3550 General Atomics Court, San Diego, California 92121[1]; Vaccine Research Center, National Institute of Allergy and Infectious Diseases, NIH, 40 Convent Drive, Bethesda, Maryland 20892[2]; Division of Viral Pathogenesis, Beth Israel Deaconess Medical Center, 330 Brookline Ave., RE-204, Boston, Massachusetts 02215[3]; National Institute for Communicable Diseases, Private Bag X4, Sandringham 2131, Johannesburg, South Africa[4]; Division of Hematology and Oncology, University of Alabama at Birmingham, 720 20th Street South, Kaul 816, Birmingham, Alabama 35294-0024[5]; Statistical Center for HIV/AIDS Research and Prevention, Fred Hutchinson Cancer Research Center, 1100 Fairview Avenue N., LE-400, Seattle, Washington 98109[6]; Department of Pathology, 9500 Gilman Drive, University of California, San Diego, California 92093[7]; Department of Surgery, Department of Molecular Genetics and Microbiology, and Duke Human Vaccine Institute, Duke University Medical Center, Durham, North Carolina 27710[8]; and Department of Pediatrics, Tulane University Medical Center, 1430 Tulane Avenue, New Orleans, Louisiana 70112[9]

Received 20 August 2008/Accepted 18 September 2008

Identifying the viral epitopes targeted by broad neutralizing antibodies (NAbs) that sometimes develop in human immunodeficiency virus type 1 (HIV-1)-infected subjects should assist in the design of vaccines to elicit similar responses. Here, we investigated the activities of a panel of 24 broadly neutralizing plasmas from subtype B- and C-infected donors using a series of complementary mapping methods, focusing mostly on JR-FL as a prototype subtype B primary isolate. Adsorption with gp120 immobilized on beads revealed that an often large but variable fraction of plasma neutralization was directed to gp120 and that in some cases, neutralization was largely mediated by CD4 binding site (CD4bs) Abs. The results of a native polyacrylamide gel electrophoresis assay using JR-FL trimers further suggested that half of the subtype B and a smaller fraction of subtype C plasmas contained a significant proportion of NAbs directed to the CD4bs. Anti-gp41 neutralizing activity was detected in several plasmas of both subtypes, but in all but one case, constituted only a minor fraction of the overall neutralization activity. Assessment of the activities of the subtype B plasmas against chimeric HIV-2 viruses bearing various fragments of the membrane proximal external region (MPER) of HIV-1 gp41 revealed mixed patterns, implying that MPER neutralization was not dominated by any single specificity akin to known MPER-specific monoclonal Abs. V3 and 2G12-like NAbs appeared to make little or no contribution to JR-FL neutralization titers. Overall, we observed significant titers of anti-CD4bs NAbs in several plasmas, but approximately two-thirds of the neutralizing activity remained undefined, suggesting the existence of NAbs with specificities unlike any characterized to date.

Broadly neutralizing antibodies (NAbs) are likely to be a key component of protective immunity conferred by an effective vaccine for human immunodeficiency virus (HIV) (26, 46, 48). However, methods for inducing NAbs that are effective against isolates characteristic of HIV type 1 (HIV-1) transmission (28, 34, 49, 53) have eluded vaccine developers thus far, despite considerable effort. NAbs generated in natural infection are invariably more effective than those elicited by vaccines. Early HIV-1 infection frequently results in highly isolate-specific NAbs that target viruses that were circulating 6 to 12 months prior to sampling rather than contemporaneous viruses, suggesting that the virus evolves to escape neutralization (9, 50, 65). Later in infection, some subjects go on to develop broadly cross-reactive NAb responses (32, 35). As this neutralizing activity perhaps best represents the type of response we would like to induce by a vaccine, efforts to understand its nature are vital.

Several conserved regions of the surface gp120 and transmembrane gp41 Env glycoproteins are potential targets for NAbs. Most important are the binding sites for the primary receptor CD4 (CD4bs) and the chemokine receptor binding site, both on gp120, and domains of gp41 involved in viral fusion with target cells, all of which need to preserve their antigenic structure to maintain viral fitness. The few neutralizing monoclonal antibodies (MAbs) isolated so far, all from infected patients, include MAb immunoglobulin G_1b12

* Corresponding author. Mailing address: Vaccine Research Center, National Institute of Allergy and Infectious Diseases, NIH, 40 Convent Drive, Bethesda, MD 20892. Phone: (301) 594-8484. Fax: (301) 480-2788. E-mail: jmascola@mail.nih.gov.

† Supplemental material for this article may be found at http://jvi.asm.org/.

▽ Published ahead of print on 24 September 2008.

(IgG_1b12), which binds an epitope that overlaps the CD4bs of gp120 MAbs; MAb 2G12, which recognizes a cluster of oligomannose residues on gp120; and MAbs 2F5, Z13, and 4E10, all of which recognize the tryptophan-rich membrane-proximal external region (MPER) of gp41 that is thought to play a key role in the fusion process. The incidence of NAbs with similar specificities and their relative contributions to broad plasma neutralization remain largely unknown. In fact, other as-yet-uncharacterized specificities could conceivably make major contributions (9).

Until quite recently, epitope-mapping methodology has been limited largely to peptide competition assays and binding assays using panels of gp120 mutants. These provide little information regarding neutralization specificity. Recently, more sophisticated methods have permitted a detailed analysis of a variety of key epitopes (2, 14, 18, 35, 69). One study (35) described the mapping of broadly neutralizing sera taken from two slow-progressing patients from a cohort infected with a well-characterized subtype B virus (39). Fractionation using gp120 immobilized on beads revealed that gp120 Abs were responsible for most of the broad neutralizing activity. Further experiments using immobilized gp120 that was either denatured or contained a mutation at residue 368 that eliminates the binding of CD4bs Abs did not effectively deplete neutralizing activity, suggesting that neutralizing CD4bs Abs were responsible for a substantial portion of the neutralizing activity in both plasmas. However, in one plasma, NAbs could be eluted from the gp120 with the mutated residue 368, suggesting that specificities distinct from the CD4bs may also contribute to the overall neutralization activity. Indeed, some of the viruses neutralized by the sera were known to be b12 resistant, further suggesting the presence of neutralizing specificities distinct from the b12 epitope.

A separate mapping study also employed gp120 fractionation to analyze the neutralizing activities in long-term nonprogressor sera from two subtype B-infected donors and one subtype A-infected donor (18). Again, gp120 Abs accounted for the neutralization of some, but not all, isolates, consistent with data from a previous analysis of one of the subtype B plasmas (14). Plasmas differed in their sensitivities to gp120 adsorption, depending on the strain from which the gp120 was generated and the virus used to test neutralization. Furthermore, a gp120 core protein exhibited a diminished ability to adsorb neutralization activity compared to the ability of a full-length gp120. In contrast, this core protein effectively adsorbed the b12 MAb. Collectively, these observations provide more evidence for the presence of CD4bs NAbs recognizing epitopes somewhat distinct from b12 that recognize structures that are absent from the gp120 core. In contrast, 2G12-competing Abs were not found in these sera. Moreover, a separate study reported weak or undetectable reactivity of HIV-1 donor sera with a gp120 outer domain fragment containing the 2G12 epitope, further emphasizing the paucity of 2G12-like Abs in natural infection (68). 2G12-competing Abs were observed in another study, however, and were more frequent in sera from long-term nonprogressors (7). It remains unclear whether these latter Abs actually contribute to neutralization or merely overlap the 2G12 epitope without neutralizing the virus.

Other mapping approaches reported to date include peptide interference assays for measuring V3 Ab-mediated neutralization (35, 36, 38) and assays employing HIV-2 in the presence of subinhibitory doses of soluble CD4 (sCD4) for measuring CD4-induced Abs (16). Gp41-specific NAbs can be measured in several ways. At a fundamental level, gp120 beads provide a way to fractionate gp41- and gp120-directed activities. Peptide interference neutralization assays provide some insight into gp41 NAbs that target the contiguous MPER region of gp41. Neutralization assays using either an HIV-2 or simian immunodeficiency virus (SIV) scaffold virus with the HIV-1 MPER region replacing the corresponding parental sequence have also been described (18, 23, 35, 69). Another assay for measuring MPER activity uses a disulfide-shackled gp120-gp41 mutant virus termed "SOS" (1, 3, 14). This virus can engage CD4 and CCR5, but fusion requires exposure to a low concentration of reducing agent to break the gp120-gp41 bridge. Only gp41 MPER NAbs can effectively neutralize the receptor-engaged intermediate (3, 14). In the few studies reported so far, little or no MPER activity was observed with most HIV-positive (HIV^+) plasmas (3, 14, 18, 35, 69). MPER epitopes, including that of 4E10, have been reported to mimic cardiolipin, and as a result, B-cell responses against this region may be regulated by immune tolerance (25), which might also explain the difficulties in formulating vaccine candidates to induce anti-MPER NAbs (26, 47, 48). However, there have been exceptional cases where relatively high MPER titers were detected in HIV-1 infections (23). Indeed, the results of an analysis of sera from a cohort of more than 200 patients whose infections were of several subtypes suggested that about one-third of HIV-1 sera have detectable levels of MPER NAbs (2). Whether the high frequency of activity observed in the latter study is attributable to the particulars of the cohort of plasmas investigated or to the exquisite sensitivity of the assay remains unclear.

The assays described to date focus entirely on known epitopes and do not account for possible NAbs that recognize quaternary trimer-specific epitopes not represented by gp120 or peptides. Recently, a native polyacrylamide gel electrophoresis (PAGE) method was described that visualizes Ab binding to Env trimers exposed on pseudovirions (12–14, 42). Only NAbs were found to bind to these trimers, confirming the role of trimer binding as a key requirement for neutralization, as suggested previously by others (19, 56). Here, we adapted this assay for mapping by employing trimers in which neutralizing epitopes were selectively eliminated by point mutations. This assay, together with a series of other mapping methods as described above, was used to comprehensively characterize a panel of 24 broadly neutralizing plasmas from subtype B- and C-infected donors.

MATERIALS AND METHODS

MAbs, sCD4, and guinea pig serum. A panel of MAbs directed to HIV-1 Env included MAb b12, directed to an epitope overlapping the CD4bs of gp120 (10); 2G12, directed to a unique glycan-dependent epitope on gp120 (55, 57); E51, directed to a CD4-inducible (CD4i) epitope on gp120 (67); 447-52D, F425, and 39F directed to the gp120 V3 loop (14, 45, 58, 60); and MAbs 2F5, Z13e1, and 4E10, directed to the gp41 MPER (44, 71). Recombinant sCD4 consisting of all four external domains was purchased from Progenics Pharmaceuticals (Tarrytown, NY). A guinea pig immune serum, WGP 102-4, was obtained by immunizing guinea pigs with a soluble BaL gp145 protein, termed B-gp145ΔCFIΔV12 (also known as 1AB subtype A), as described previously (66). This 1AB subtype A protein had been modified to eliminate the gp120/gp41 cleavage site, fusion

peptide, the interhelical gp41 connector, and the V1 and V2 loops. The native BaL V3 sequence was also replaced with a subtype A V3 loop that was truncated at the stem.

Human plasmas. HIV-1 donor plasmas were obtained from various subtype B- and C-infected donors. One subtype B plasma, LT2, also known as N308, came from a long-term nonprogressor described previously (14, 18). Seven other subtype B plasmas, from United States donors 1648, 1652, 1685, 1686, 1687, 1688, and 1702, were obtained from Zeptometrix Corporation (Buffalo, NY). The patients were attending clinics enrolling patients for apheresis, and the samples obtained therefore correspond to the time of initial diagnosis. Two HIV-negative control plasmas, 210 and 211, were also obtained from Zeptometrix.

Plasmas from sixteen subtype C donors were purchased from the South African Blood Bank (Johannesburg) and were selected from an initial panel of plasmas from 107 donors, some of which have been described previously (23, 34). Like the commercial subtype B plasmas, these subtype C plasmas are likely to be from the first diagnosis of chronic infection. Clinical information was unavailable because of the policy of anonymity of Blood Bank material. The entire panel will be described in detail in a separate article (E. Gray and L. Morris, unpublished data).

Enzyme-linked immunosorbent assay (ELISA). Recombinant consensus gp140 (CONS gp140CFI) oligomers (provided by H. X. Liao and B. F. Haynes) (21, 37) and gp41 (Immunodiagnostics, Inc.) were precoated overnight onto microtiter wells (NUNC) and washed with an automated plate washer (Bio-Tek). For IgA and IgM detection, IgG was first absorbed out by protein G columns (protein G MultiTrap; GE Healthcare). Plasmas were then diluted and incubated with the immobilized antigens on the microwells. The plates were washed and then probed with subclass-specific anti-human Ig conjugated to alkaline phosphatase (anti-IgG1, anti-IgG2, anti-IgG3, anti-IgG4, and anti-IgM from Southern Biotech and anti-IgA from Jackson ImmunoResearch Laboratories). These conjugates were tested for specificity and chosen based on their on lack of cross-reactivity. Optical density (OD) readings at 410 nm were measured by using a VersaMax plate reader (Molecular Devices), and an average OD reading for each pair of replicates, with the background subtracted, was calculated. For each test, duplicate antigen-containing and blank wells were examined. A score (i.e., OD of antigen − OD of nonantigen) was positive if greater than or equal to an OD of 0.1 after the background was subtracted. A standardized HIV+ positive control was titrated in each assay (tracked with a Levy-Jennings plot with acceptance of titer only within 3 standard deviations of the mean), and the average OD was plotted as a function of plasma dilution to determine the Ab titer using a four-parameter logistic equation (SoftMax Pro; Molecular Devices). The concentration of isotype- and subclass-specific Ab was calculated by linear regression using a concentration curve of purified IgG1, IgG2, IgG3, IgG4, IgA, or IgM proteins (Sigma) in each plate, allowing a comparison of the relative levels of plasma Abs. The two negative-control plasmas (210 and 211) were included in each assay to ensure specificity, consistency, and reproducibility. The controls for the detection of HIV-1-specific IgM Abs included a test for rheumatoid factor. The integrity of raw data acquisition and data analysis was electronically tracked (21 CFR part 11 compliant).

Live HIV-1, HIV-2, and SIV viral isolates and pseudoviruses. Live viral stocks and Env pseudotypes of various isolates were generated for neutralization assays. Pseudoviruses were produced by cotransfection of 293T cells with an Env-expressing plasmid and one of two Env-deficient HIV-1 genomic backbone plasmids, pNL-LucR-E- (for CF2 neutralization assays) or pSG3ΔEnv (for TMZ-bl neutralization assays) (3, 33, 34). A repertoire of Env plasmids included subtype B and C tier 2 reference strains (33, 34). Several other Env plasmids and virus stocks have been described previously (3, 35, 59). The SHIV-89.6P and SHIV-SF162P3 viruses were uncloned live viruses grown on human peripheral blood mononuclear cells (PBMCs) (24). A mutant JR-FL Env plasmid was generated, JR-FL.d301, with an asparagine-to-glutamine exchange at position 301, resulting in the removal of an N-linked carbohydrate moiety. Tier 1 virus plasmids for SF162.LS and MW965.26 Envs (11) were obtained from L. Stamatatos (Seattle Biomedical Research Institute) (61) and the NIH AIDS Reference and Reagent Program (originally provided by B. Hahn) (20), respectively. Chimeric HIV-2 Envs containing various segments of the HIV-1 MPER (see Fig. S3 in the supplemental material) were constructed from a parental HIV-2/7312A plasmid (2, 23). An Env plasmid expressing another HIV-2 isolate, KR, has been described elsewhere (K. L. Davis, F. Bibollet-Ruche, H. Li, J. M. Decker, O. Kutsch, L. Morris, A. Strenger, A. Pinter, J. A. Hoxie, B. H. Hahn, P. D. Kwong, and G. M. Shaw, submitted for publication). The SIVmac239CS.23 Env plasmid was subcloned from an animal challenge stock of molecularly cloned SIVmac239/nef-open provided by R. Desrosiers.

Neutralization assays. Neutralization assays were performed using either TZM-bl or CF2 target cells. Each assay was performed in duplicate and repeated at least twice.

(i) Neutralization assays using TZM-bl target cells. The single-cycle TZM-bl neutralization assay has been described previously (33). To determine the plasma-neutralizing 50% infective dose (ID_{50}), serial dilutions of heat-inactivated plasma or MAb were incubated with virus and the neutralization dose-response curves were fitted by nonlinear regression using a four-parameter hill slope equation.

In peptide interference neutralization assays, a control or test peptide was added to the plasma 30 min prior to the addition of virus. The final concentration of peptide in mixtures with plasma and virus was 25 μg/ml, except for peptide 4E10.22, which was used at a concentration of 12.5 μg/ml (36). To control for possible direct effects of peptides on infection (i.e., in the absence of MAb or plasma), assays were conducted in the presence of peptides at the same concentrations as those used in interference assays. In these experiments, the peptides had either little or no effect on virus infectivity. This internal control level of infection with each peptide was used as a baseline reference for peptide competition assays with plasmas. The MPER and V3 loop-based peptides based on the YU2 and TV1 isolates are depicted in Fig. S3 and S6 in the supplemental material and were synthesized by Biosynthesis (Lewisville, TX) and solubilized in dimethyl sulfoxide and water.

(ii) Neutralization assays using CF2 target cells. Neutralization assays using canine CF2 cell lines in standard and post-CD4/CCR5 formats have been described previously (3, 14). Briefly, in the standard format, virus was incubated with graded dilutions of Ab for 1 h at 37°C. The mixture was then added to CF2 cells, spinoculated, and incubated for 2 h at 37°C, after which the medium was changed. After 3 days of culture, luciferase activity was measured. Post-CD4/CCR5 binding neutralization was measured using SOS mutant particles (1, 3). The particles were allowed to attach to target cells for 2 h, after which unbound particles were washed away and graded concentrations of Abs were added for 1 h. Infection was then activated by using 5 mM dithiothreitol for 10 min to reduce the gp120-gp41 disulfide bond (SOS), allowing infection to proceed.

Plasma fractionation using paramagnetic-bead-immobilized gp120. Plasma fractionation by using paramagnetic bead-immobilized gp120 has been described previously (35). The two forms of YU2 gp120 used were the parental wild type (WT) and a D368R mutant gp120 that eliminates the binding of most known Abs to the CD4bs. Beads coated with bovine serum albumin (purchased from Sigma) and blank beads were used as controls. Briefly, each protein was covalently coupled to 1.1 μM *p*-toluenesulfonyl (tosyl)-activated paramagnetic beads (MyOne tosylactivated Dynalbeads; Invitrogen) according to the manufacturer's instructions. Beads were used at a concentration of 40 mg/ml. Generally, 40 mg of beads was reacted with 2 mg of protein. The antigenic integrity of each protein after bead coupling was verified by flow cytometry using known MAbs b12, 2G12, 447-52D, 17b, and polyclonal HIV Ig. For adsorptions, plasmas were diluted to between 1:20 to 1:30 in Dulbecco's modified Eagle's medium (DMEM)–10% fetal bovine serum and 800 to 1,000 μl of diluted plasma was incubated with 400 to 500 μl of beads at room temperature for 30 min. Beads were separated with a magnet, centrifuged, separated from the supernatant, and stored in phosphate-buffered saline (PBS)–0.2% bovine serum albumin–0.02% sodium azide buffer at 4°C. The adsorbed plasma supernatant was then characterized in ELISAs and neutralization assays. To elute functional Abs from beads, the beads were first washed in PBS containing 500 mM NaCl and then exposed to a series of increasingly acidic conditions. The following elution procedure was determined from optimization experiments to effectively elute bound Ab while maintaining its functional neutralizing activity. Beads were first reacted with a 100 mM glycine-HCl elution buffer (pH 2.7) for 30 s during vortexing and then pelleted by centrifugation and held in place with a magnet; the separated IgG was removed and placed into a separate tube where the pH was adjusted to between pH 7.0 and 7.4 with 1 M Tris (pH 9.0) buffer. The eluted IgG was then diluted in DMEM, washed over a 30-kDa Centricon plus filter (Millipore Corp.), and resuspended in DMEM. The beads were exposed to a glycine-HCl buffer at a pH of 2.3 and then at pH 1.7. After all three elutions, the eluted IgG fractions were combined. The concentration of IgG was measured by using a commercial radial immunodiffusion kit (Binding Site Corp.). Neutralization data were processed as follows: if the unbound fractions from adsorptions against blank, WT gp120, and D368R mutant gp120 beads are assigned as a, b, and c, then the percent gp120-directed activity = $[(a - b)/a] \times 100$ and the percent CD4bs activity of the total neutralization = $[(c - b)/a] \times 100$.

Native PAGE trimer shifts. Blue native PAGE (BN-PAGE) band shifts were used to analyze Ab binding to native, virion-derived Env trimers as described previously (12–14, 42). Briefly, concentrated JR-FL SOS pseudovirions were mixed with graded amounts of MAbs, plasmas, or sCD4 for 5 min. The particles

			clade B				clade C														controls		geometric
Virus	Clade	Location	1648	1652	1686	1702	BB8	BB12	BB14	BB21	BB24	BB28	BB34	BB47	BB55	BB68	BB75	BB80	BB81	BB87	BB105	BB107	210	211	mean ID50*
SF162.LS	B	USA	3,991	1,307	7,032	4,316	8,330	4,675	15,056	11,972	4,750	2,164	27,212	1,686	8,339	1,660	7,111	7,125	712	8,984	10,625	13,714	<20	<20	5,330
HXB2	B	France	278	1,109	314	424	1,634	6,070	1,744	2,374	2,946	10,101	17,288	5,717	3,743	1,171	5,418	2,651	1,513	9,742	1,429	332	<20	<20	2,071
Bal.26	B	USA	533	375	934	1,493	498	460	903	559	255	130	798	235	499	153	160	346	154	747	405	1,399	<20	<20	434
6535.3	B	USA	143	311	120	257	408	858	349	321	626	197	306	214	605	140	107	517	145	1,269	315	2,691	<20	<20	335
JR-FL d301	B	USA	188	361	1,914	1,102	110	64	n.d.	n.d.	n.d.	n.d.	n.d.	n.d.	159	n.d.	495	n.d.	131	1,120	199	496	<20	<20	320
RHPA4259.7	B	USA	141	112	503	149	258	728	354	426	177	1,029	192	366	175	152	101	182	210	457	219	883	<20	<20	269
AC10.0.29	B	USA	425	267	119	162	275	520	403	281	284	142	370	216	460	218	118	253	205	504	331	1,120	<20	<20	286
REJO4541.67	B	USA	619	870	217	624	320	126	324	670	115	116	331	199	93	224	43	99	97	268	425	158	<20	<20	222
SHIV-89.6P	B	USA	441	335	172	448	313	389	180	312	155	80	131	136	207	144	91	224	93	332	290	900	<20	<20	222
WITO4160.33	B	USA	106	780	204	392	293	277	389	237	307	126	243	238	193	133	95	168	141	307	307	146	<20	<20	222
SS1196.1	B	USA	146	178	187	367	161	298	509	189	211	53	416	258	363	80	125	176	90	804	136	145	<20	<20	198
SC422661.8	B	Trinidad	203	201	121	150	197	289	250	224	246	97	800	240	210	140	130	130	162	408	180	140	<20	<20	198
JR-FL	B	USA	40	143	1,329	192	131	413	40	35	20	35	292	100	100	20	150	50	80	600	70	600	<20	<20	110
TRO.11	B	Italy	110	130	195	171	564	476	66	251	66	72	250	80	200	73	41	331	61	404	101	519	<20	<20	153
CAAN5342.A2	B	USA	263	180	110	125	199	175	157	338	201	81	150	305	229	104	71	108	96	527	303	279	<20	<20	175
THRO4156.18	B	USA	262	259	138	173	180	89	213	409	171	105	131	207	239	109	50	131	85	132	140	88	<20	<20	148
SHIV-SF162.P3	B	USA	237	315	138	243	155	126	115	226	115	88	66	56	94	75	38	85	64	146	139	453	<20	<20	123
TRJO4551.58	B	USA	99	55	83	316	155	172	77	182	50	735	73	73	33	54	58	91	36	109	84	30	<20	<20	89
QH0692.42	B	Trinidad	117	216	124	114	65	204	64	48	120	44	110	91	63	65	75	94	75	167	65	57	<20	<20	89
PVO.4	B	Italy	67	97	141	118	38	225	31	54	50	40	38	55	76	32	26	31	35	41	44	93	<20	<20	55
geometric mean ID50 (clade B)*			**180**	**224**	**196**	**245**	**206**	**285**	**179**	**218**	**141**	**111**	**203**	**155**	**173**	**96**	**77**	**142**	**95**	**319**	**170**	**293**	**<20**	**<20**	**179**
MW965.26	C	Malawi	5,619	3,011	2,375	2,186	25,388	12,353	110,682	98,928	80,906	15,271	461,999	21,189	33,569	11,606	12,016	14,707	4,061	42,052	11,813	12,002	<20	<20	17,346
CAP45.2.00.G3	C	S. Africa	922	995	153	394	480	1,514	749	578	494	1,420	768	1,024	478	1,126	109	1,050	446	1,175	1,855	203	<20	<20	636
Du151.2	C	S. Africa	64	60	72	108	98	998	423	177	378	160	102	193	616	62	9,320	302	102	336	152	1,076	<20	<20	229
Du156.12	C	S. Africa	380	358	149	333	242	666	175	93	299	154	1,263	328	389	254	312	349	258	957	217	761	<20	<20	323
ZM135M.PL10a	C	Zambia	422	353	128	171	433	372	479	651	483	142	1,056	360	444	317	200	325	296	487	539	287	<20	<20	352
CAP210.2.00.E8	C	S. Africa	546	228	171	313	471	269	562	632	627	267	329	733	408	253	145	259	416	433	470	224	<20	<20	353
ZM233M.PB6	C	Zambia	146	190	86	156	434	230	369	327	596	272	269	786	462	231	148	419	725	1,222	341	160	<20	<20	305
ZM214M.PL15	C	Zambia	2,028	390	132	470	359	382	142	209	483	233	268	414	204	220	113	154	271	291	261	71	<20	<20	265
ZA012	C	Zambia	n.d.	n.d.	n.d.	n.d.	n.d.	n.d.	n.d.	n.d.	n.d.	168	382	n.d.	n.d.	50	1,081	n.d.	n.d.	n.d.	11	n.d.	n.d.	n.d.	131
ZM109F.PB4	C	Zambia	282	185	183	320	467	280	472	685	395	136	384	501	363	253	133	236	213	336	285	249	<20	<20	291
ZM249M.PL1	C	Zambia	296	161	227	568	270	172	255	378	398	263	141	391	222	169	120	168	417	490	312	159	<20	<20	254
ZM197M.PB7	C	Zambia	414	402	141	276	274	137	375	348	302	126	877	275	271	167	83	160	148	155	218	92	<20	<20	221
Du172.17	C	S. Africa	35	99	39	86	298	954	167	105	230	288	94	551	195	95	232	297	231	428	138	248	<20	<20	176
TV1.29	C	S. Africa	96	69	22	123	192	185	93	170	247	127	286	462	264	158	137	161	131	274	178	136	<20	<20	150
ZM53M.PB12	C	Zambia	232	112	209	247	230	82	138	275	115	286	68	201	131	258	35	114	77	83	151	104	38	<20	138
Du422.1	C	S. Africa	<20	31	36	55	92	221	170	147	99	112	89	305	113	251	30	224	167	140	120	487	<20	<20	105
Du123.6	C	S. Africa	98	118	56	103	60	210	64	73	186	77	226	158	109	112	133	106	118	258	82	237	<20	<20	116
geometric mean ID50 (clade C)*			**203**	**175**	**99**	**203**	**250**	**321**	**248**	**255**	**314**	**198**	**283**	**390**	**273**	**190**	**178**	**240**	**223**	**363**	**206**	**224**	**<20**	**<20**	**225**
overall geometric mean ID50*			**190**	**199**	**142**	**224**	**225**	**301**	**209**	**235**	**205**	**147**	**239**	**239**	**214**	**133**	**115**	**181**	**142**	**339**	**187**	**258**	**<20**	**<20**	**200**
SIVmac239CS.23			<20	<20	<20	<20	<20	<20	<20	<20	<20	<20	<20	<20	<20	<20	<20	<20	<20	<20	<20	<20	<20	<20	
HIV-2 KR			<500	<500	<500	<500	<20	<20	<20	<20	<20	<20	<20	<20	<20	<20	<20	<20	<20	<20	<20	<20	<20	<20	
HIV-2 7312A			<20	166	25	100	<20	<20	<20	<20	26	<20	<20	27	<20	<20	<20	<20	<20	52	<20	<20	<20	<20	

FIG. 1. Breadth and potency of neutralization by a panel of subtype B and C plasmas. Four of the 8 subtype B and all 16 subtype C plasmas, organized horizontally, were evaluated in the TZM-bl neutralization assay, with the exception of JR-FL neutralization that was determined in the CF2 assay. A panel of subtype B and C viruses are organized in the top and bottom halves of this figure, respectively, and control HIV-2 and SIV viruses are shown at the bottom. Subtype B and C viruses are arranged with those for the most-sensitive tier 1 isolates at the top and the most-resistant tier 2 isolates at the bottom, as shown by calculations of the geometric mean titers in the rightmost column. The country of origin of each Env, where known, is indicated in the third column. ID_{50} titers are color coded as follows: white boxes, titer <20; green boxes, titer <100; yellow boxes, titer <500; orange boxes, titer <1,000; and red boxes, titer >1,000. *, calculations of geometric mean titers took into account values against all isolates except the overtly sensitive JR-FL.d301, SF162.LS, HXB2, and MW965.26 viruses. n.d., not done.

were then washed with PBS and gently solubilized in 0.12% Triton X-100 in 1 mM EDTA–1.5 M aminocaproic acid and one microliter of a protease inhibitor cocktail (Sigma). An equal volume of 2× sample buffer containing 100 mM morpholinepropanesulfonic acid (MOPS), 100 mM Tris-HCl, pH 7.7, 40% glycerol, and 0.1% Coomassie blue was then added. Samples were then loaded onto a 4-to-12% *N*,*N*-methylenebisacrylamide-Tris NuPAGE gel (Invitrogen), using ferritin (Amersham) as a size standard, and were electrophoresed at 4°C for 3 h at 100 V with 50 mM MOPS–50 mM Tris, pH 7.7, containing 0.002% Coomassie blue as the cathode buffer and the same buffer without Coomassie blue as the anode buffer. The gel was then blotted onto polyvinylidene difluoride, destained, transferred to blocking buffer (4% nonfat milk in PBS), and probed with MAbs b12, 2G12, E51, 39F, 2F5, and 4E10, followed by an anti-human Fc alkaline phosphatase conjugate (Jackson). Trimer binding was measured via a depletion of the unliganded trimer using UN-SCAN-IT densitometry software (Silk Scientific) (12). Briefly, ID_{50}s were calculated with reference to the control lanes in each gel, in which the density of a uncomplexed control trimer band is taken as 100% and one that is fully liganded by NAb (either b12, 2G12, or a high concentration of plasma) is taken as 0%. The experiments were run a minimum of three times to confirm the accuracy of the 50% inhibitory concentration (IC_{50}) estimates. The molecular masses of trimer-Ab complexes were estimated relative to the estimated molecular masses of 420 and 140 kDa for JR-FL gp160ΔCT trimers and monomers, respectively (12).

Virus capture competition. In virus capture assays (13, 17, 42), MAbs were coated onto ELISA microwells overnight at 5 μg/ml. The wells were then washed and blocked with 3% bovine serum albumin in PBS. Graded dilutions of Abs were added to JR-FL pseudoviruses bearing surface vesicular stomatitis virus G. These virus-Ab mixtures were then added to MAb-coated ELISA wells for 3 h, followed by washing with PBS. For E51 MAb capture, a fixed concentration of 5 μg/ml sCD4 was added throughout. CF2-CD4/CCR5 cells (29) were then overlaid, and 2 days later, the level of infection was measured by assaying luciferase. The reciprocal plasma dilution that inhibited MAb-mediated virus capture by 50% was recorded.

RESULTS

Identification of broadly neutralizing plasmas from donors chronically infected with HIV-1 subtypes B and C. Preliminary screening of the neutralizing activity of a panel of 27 subtype B plasmas against five primary isolates was performed by Monogram BioSciences using the PhenoSense assay (5). This led to the selection of seven with considerable neutralization breadth. Together with the broadly neutralizing subtype B plasma, LT2, these made up our panel of eight neutralizing subtype B plasmas. A similar screening of 107 subtype C plasmas against seven subtype C and three subtype B primary viruses led to the selection of 14 with the greatest neutralization breadth and 2 more (BB21 and BB81) with moderate breadth.

To provide a frame of reference for mapping studies, we initially assessed the neutralization activities of these selected plasmas against a panel of 40 viruses, including 20 subtype B, 17 subtype C, and HIV-2 and SIV controls (Fig. 1). Insufficient quantities of the other four subtype B plasmas, 1685, 1688, 1687, and LT2, were available to include them in this analysis. However, the results of a separate investigation of these plasmas show that their neutralization titers against a separate panel of mostly subtype B, C, and AE viruses are comparable to those of the other plasmas shown in Fig. 1 (J. M. Binley, T. Wrin, and D. Burton, unpublished data). An analysis of plasma LT2's neutralization breadth has also been published previ-

ously (18). The panel of viruses used for the assays whose results are shown in Fig. 1 included those used in the mapping analyses described below and subtype B and subtype C tier 2 reference panel viruses described previously (33, 34).

Inspection of the rows in Fig. 1 reveals the inherent sensitivities of each virus, providing context for each value in reference to the larger data set. The viruses are organized with the most sensitive at the top of each subtype (see right-hand column of Fig. 1). As expected, all the HIV+ plasmas effectively neutralized the tier 1 sensitive isolates SF162, HXB2, and MW965.26. The subtype B plasmas neutralized the d.301 JR-FL virus somewhat more potently than the JR-FL parent. This mutant lacks a carbohydrate moiety that protects the V3 loop in the parental version. Conversely, the subtype C plasmas neutralized these two viruses with largely equivalent titers. Subtype differences were even more apparent for neutralization of the MW965.26 isolate, which was neutralized with an average titer of 1:60,534 by subtype C plasmas but only 1:3,298 by the subtype B plasmas. Collectively, this suggests some subtype-based preference in the neutralization of certain isolates. However, this idea is complicated by the relatively potent neutralization of the subtype B isolate HXB2 and, to a lesser extent, SF162.LS by the subtype C plasmas.

The columns in Fig. 1 reveal the potency and breadth of plasma neutralization. Importantly, all the plasmas neutralized the tier 2 reference viruses. The geometric mean ID_{50}s ranged from 1:133 to 1:339, excluding negative controls, the d.301 JR-FL mutant, and the SF162, HXB2, and MW965.26 viruses. Despite the general breadth of neutralization observed in Fig. 1, varied neutralization titers against the refractive primary isolate JR-FL were observed. For example, plasma 1686's titer of 1:1,329 against JR-FL was significantly higher than its geometric mean titer of 1:142. This activity is important, as we focus most of our attention on JR-FL in our attempts to dissect the specificities contributing to neutralization. Although we did not observe clear subtype-restricted patterns against tier 2 viruses (8), on average, intrasubtype neutralization was slightly more potent than intersubtype neutralization, particularly for some subtype C plasmas. By using generalized estimating equations to evaluate intra- versus interclade neutralization, excluding tier 1 and sensitive isolates, subtype B plasmas neutralized matched-subtype viruses 1.28-fold ($P = 0.3$) more potently and subtype C plasmas neutralized them 1.53-fold ($P = 0.015$) more potently. Notably, the subtype B plasmas did not neutralize the Durban subtype C viruses as effectively as the other subtype C viruses, while subtype C plasmas did not appear to discriminate between these and other subtype C Envs. However, the P values for these differences are, at best, marginally significant ($P = 0.3$ and $P = 0.02$, respectively, using generalized estimating equations of linear regression and factoring the correlation between multiple plasmas values for each virus).

Neutralizing activity against the SIV and the HIV-2 KR control viruses was undetectable, as expected. However, weak activity against the HIV-2 7312A isolate was detected in some cases, particularly subtype B plasmas 1652 and 1702. This activity probably stems from Abs directed to a CD4i epitope that is partially conserved between HIV-1 and HIV-2 isolates (16).

Collectively, the data shown in Fig. 1 suggest that any attempt to map neutralization is likely to be constrained by the coexistence of broadly cross-reactive NAbs and NAbs with little cross-reactivity. However, mature anti-gp120 Ab responses have been reported to be oligoclonal rather than polyclonal (15), providing some hope regarding the practicality of attempts to deconvolute the neutralizing activity and the feasibility of fine mapping of polyclonal plasma neutralization.

ELISA binding of Gp41 and gp140 by different IgG subclasses and IgA. To profile the distribution of Env-specific Abs, we assessed the reactivities of the IgG1, IgG2, IgG3, and IgG4 isotypes and IgA and IgM subclasses to a consensus gp140 Env glycoprotein. Fig. S1 in the supplemental material shows a box plot of the relative distribution of Ab types present in plasmas. All plasmas had detectable IgG1 and IgA, but IgG2, IgG3, IgG4, and IgM were detected less frequently. The heavily biased IgG1 profile (see Fig. S1 in the supplemental material; similar gp41 data are not shown) was perhaps consistent with a Th2-like response, typical of HIV-1 infection. There were no observable differences in isotype or subclass responses between the subtype B and C plasmas. However, the individual plasmas that scored positive for either anti-gp140 IgG2 or IgG3 were discordant, suggesting differences in the regulation or stimulation of these Abs. Anti-gp140 IgA Abs were detectable in all the plasmas, but the relative concentration was significantly lower than the level of IgG1 (median, 3 μg/ml versus 94 μg/ml; Student's t test, $P < 0.001$).

Plasma fractionation using WT and CD4bs knockout mutant YU2 gp120 beads. For the purpose of the mapping analyses, we used the subtype B isolate JR-FL as a common prototype virus. The basis for this choice is that it has been a widely used primary isolate in the field. In addition, the gp120/gp41 cleavage site of JR-FL Env is effectively processed and trimers are expressed efficiently, both of which are important advantages for the native PAGE assay described below.

To determine the contribution of gp120 Abs to JR-FL neutralization, plasmas from four subtype B- and four subtype C-infected individuals were adsorbed with WT YU2 gp120 covalently linked to paramagnetic beads (35). Plasmas were also fractionated on beads coupled to a YU2 gp120 with a D368R mutation that is known to exclude the binding of most CD4bs Abs (35, 51). The efficiencies of gp120 adsorptions were verified by the results of WT gp120 and D368R protein ELISAs which demonstrated that each gp120 adsorbed all, or nearly all, detectable binding Abs to the corresponding gp120 (data not shown). However, adsorption with the D368R mutant left variable amounts of WT gp120 binding activity in some plasmas. This residual gp120 binding most likely represented CD4bs-specific Abs that were not adsorbed by the gp120 mutant.

We next assessed the neutralizing activities of the WT- and D368R-gp120-adsorbed plasmas. Assays were performed with other subtype B and C viruses in many cases, as well as the JR-FL prototype virus, to accommodate the possibility that the specificities by which the JR-FL isolate is neutralized may differ from those that neutralize other primary isolates of subtype B or other subtypes. We did not use the YU2 virus in neutralization assays, as we are interested in assessing broad neutralizing activity rather than any strain-specific activity directed to the matched YU2 isolate. The raw titrations shown in Fig. 2 show the neutralizing ID_{50}s after adsorption with beads linked to WT or D368R gp120 or blank control beads, and the

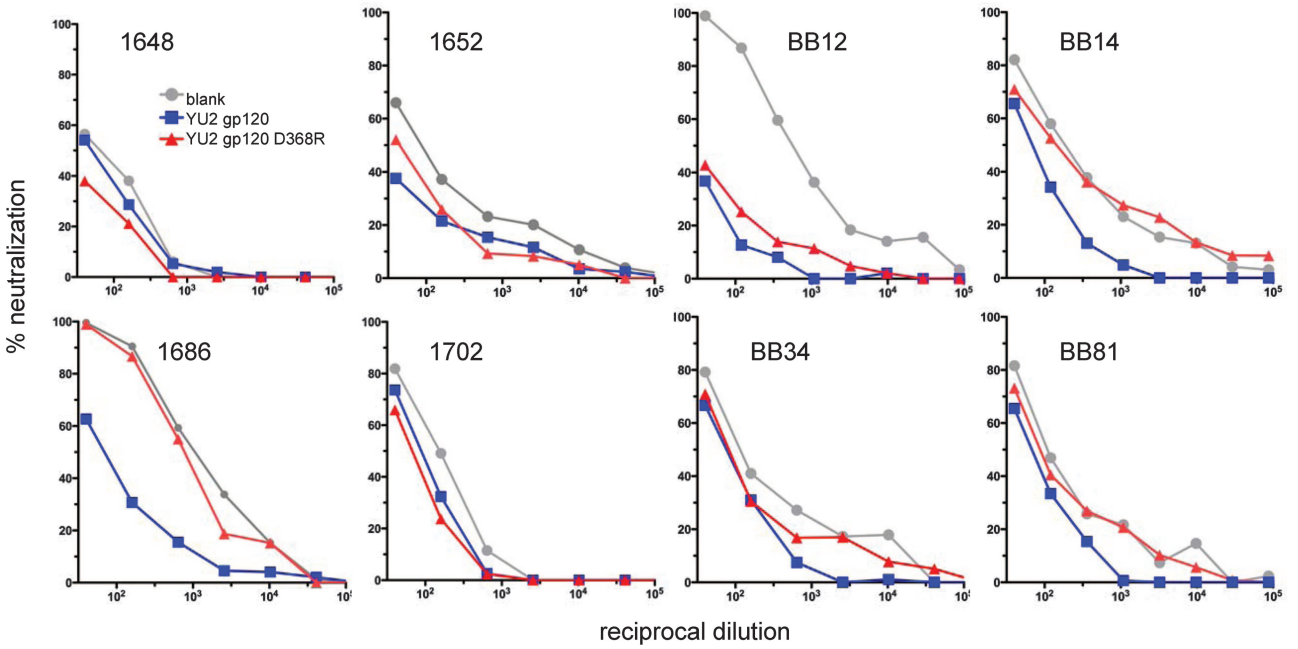

FIG. 2. Neutralization analysis of plasmas fractionated on gp120 beads. Plasmas were fractionated on YU2 WT gp120, D368R gp120, or blank (control) beads. JR-FL neutralization assays were performed on unbound fractions using the TZM-bl assay.

data are summarized in Fig. 3. The percentages of gp120-directed Abs (Fig. 3) were determined by comparing ID_{50} values after blank- and WT-gp120-bead adsorption. For example, the reciprocal ID_{50} titers for plasma 1686 against JR-FL were 1,185 (blank beads) and 70 (WT gp120 beads), respectively, and therefore 94% {[(1,185 − 70)/1,185] × 100} of JR-FL neutralization was removed by WT gp120 (Fig. 2 and 3). The percentage of gp120-directed neutralization varied depending on the virus isolate used in the neutralization assays. In most cases, the neutralization of tier 1 HXB2 and SF162 viruses was predominantly gp120 directed, but the percentages of gp120-directed neutralization of JR-FL and other primary viruses varied considerably. Plasma 1686 was exceptional, however, in that more than 80% of the neutralization activity against all viruses tested, including a subtype A and a subtype C virus, was removed by the subtype B YU2 WT gp120, suggesting the presence of NAbs predominantly directed to a conserved region of gp120. In comparison, the gp120-directed neutralization mediated by the three other subtype B plasmas was more varied. For plasmas 1648 and 1702, less than one-half of the JR-FL neutralization activity was adsorbed by YU2 WT gp120 (Fig. 2 and 3), suggesting the presence of residual neutralizing activity against gp41, putative quaternary trimer epitopes, or strain-specific epitopes that are not available on YU2 gp120.

The percentage of CD4bs NAbs was calculated by comparing the neutralization activity remaining after WT gp120 adsorption (i.e., all remaining non-gp120 activity) to that remaining after D368R mutant adsorption (i.e., all non-gp120 plus any CD4bs activity). For example, in considering the plasma 1686 neutralization of JR-FL (Fig. 2 and 3), 61% of the total activity was directed to the CD4bs, calculated by the difference between the residual neutralization titers after WT gp120 and residue 368 mutant adsorptions divided by the total activity [i.e., (797 − 70/1,185) × 100]. This calculation was only performed in cases where >50% of the plasma's neutralizing activity was directed to gp120. The percent of gp120 neutralization activity that was CD4bs directed can also be calculated simply as the total CD4bs activity (61%) divided by the fraction of gp120 activity calculated above (94%), giving a value of 65%.

We noted above that plasma 1686 had an especially high neutralization titer against JR-FL (Fig. 1). The results of previous studies indicate that JR-FL is highly sensitive to MAb b12, suggesting the possibility that b12-like CD4bs Abs may be present in this plasma, as the results of our mapping studies here indicate. Plasma 1686 also clearly neutralized five of the seven viruses tested via the CD4bs, suggesting broad CD4bs specificities, effective even against subtype C viruses (Fig. 3). The exceptions, HXB2 and SF162, were not significantly neutralized through the CD4bs, suggesting that these tier 1 viruses were predominantly neutralized by other specificities, perhaps V3 loop or CD4i Abs that do not effectively neutralize the more-resistant tier 2 viruses. To further confirm the predominantly CD4bs-directed neutralization by the 1686 plasma, we assessed the activities of Abs that were eluted from WT and D368R gp120. Consistent with the above observations, the Abs eluted from D368R gp120 (lacking CD4bs Abs), were 10-fold less potent than the Abs eluted from WT gp120 beads (see Fig. S2 in the supplemental material).

The remaining subtype B plasmas we evaluated in this assay contained assorted amounts of gp120-directed activity and little CD4bs-directed activity. All three neutralized the sensitive virus SF162 predominantly via gp120-directed Abs. In contrast, neutralization activity against the more-resistant JR-FL was not so easily adsorbed by gp120, with only plasmas 1686 and

plasma ID	virus	subtype	ID50 blank	ID50 gp120 wt	ID50 gp120 D368R	% gp120-directed	% CD4bs-directed
1648	HXB2	B	354	20	40	**94%**	6%
	SF162	B	1330	173	150	**87%**	0%
	BaL.01	B	63	40	20	37%	
	JR-FL	B	64	51	40	20%	
1652	HXB2	B	1080	531	1105	**51%**	**51%**
	SF162	B	615	249	280	**60%**	5%
	BaL.01	B	55	40	20	27%	
	JR-FL	B	93	20	43	**78%**	**25%**
1686	HXB2	B	408	40	40	**90%**	0%
	SF162	B	928	158	93	**83%**	0%
	BaL.01	B	1069	40	778	**96%**	**69%**
	JR-FL	B	1185	70	797	**94%**	**61%**
	RHPA	B	365	40	456	**89%**	**89%**
	RW020	A	121	20	104	**83%**	**69%**
	ZM249M	C	432	40	174	**91%**	**25%**
1702	HXB2	B	456	284	320	38%	
	SF162	B	804	182	141	**77%**	0%
	BaL.01	B	161	130	95	19%	
	JR-FL	B	146	88	66	40%	
BB12	HXB2	B	982	61	807	**94%**	**76%**
	SF162	B	2144	80	219	**96%**	7%
	JR-FL	B	676	20	20	**97%**	0%
	Du151	C	2285	166	362	**93%**	7%
	Du156	C	859	185	367	**78%**	21%
BB14	HXB2	B	2666	56	1820	**98%**	**67%**
	SF162	B	769	60	276	**92%**	**28%**
	JR-FL	B	218	69.3	166	**68%**	**44%**
	Du151	C	739	285	525	**61%**	**32%**
	Du156	C	281	140	274	**50%**	**48%**
BB34	HXB2	B	9426	2592	6364	**73%**	**40%**
	SF162	B	2304	174	362	**92%**	8%
	JR-FL	B	160	76	88	**53%**	7%
	Du151	C	174	81	133	**54%**	**30%**
	Du156	C	605	645	673	0%	
BB81	HXB2	B	671	130	463	**81%**	**50%**
	SF162	B	458	123	249	**73%**	**28%**
	JR-FL	B	139	68.9	106	**50%**	**27%**
	Du151	C	145	88	175	39%	
	Du156	C	441	375	302	15%	

FIG. 3. Summary of plasma fractionation on gp120 beads. Plasmas at a 1:20 dilution were adsorbed to blank or gp120 beads and then tested in TZM-bl neutralization assays, causing a further twofold dilution, giving a final starting dilution of 1:40. Reciprocal neutralization ID_{50} titers are shown. In cases where no neutralization was observed at 1:40, a value of 20 is given. Fourth column, plasmas adsorbed on untreated tosyl-activated Dynabeads; fifth column, plasmas adsorbed with WT YU2 gp120; sixth column, plasmas adsorbed with D368R YU2 gp120 (CD4bs knockout mutation); seventh column, percent reduction in total neutralizing ID_{50} by WT gp120 adsorption relative to that of blank beads. In cases where the WT titer was higher than that of the blank, a value of 0% was assigned; in cases where gp120-directed activity was >50% of the total neutralizing titer, the contribution of CD4bs activity was calculated. Eighth column, CD4bs-directed activity expressed as the percentage of the total neutralization titer. Values in bold are considered significant; i.e., cases where gp120 adsorbs >50% of total neutralizing activity and >25% of the activity is directed to the CD4bs. The calculations underlying these percentages are described in Materials and Methods.

1652 demonstrating a majority fraction of gp120-directed neutralization (Fig. 2 and 3).

Like the subtype B plasmas, the subtype C plasmas displayed various levels of gp120-directed neutralization. The subtype B YU2 WT gp120 protein beads adsorbed the majority of the neutralizing activity from plasmas BB12 and BB14 against both subtype B and C viruses, suggesting NAbs directed to conserved regions of gp120. However, these beads were somewhat less efficient at adsorbing the neutralizing activity from plasmas BB34 and BB81. While much of the neutralization of subtype B viruses HXB2 and SF162.LS was gp120 directed, relatively large proportions of the neutralizing activities against subtype C viruses Du151 and Du156 remained after WT gp120 adsorption. Thus, the specificities in plasmas BB34 and BB81 that mediate neutralization of these two primary C viruses remain undefined.

Fractionation of subtype C plasmas on WT and D368R gp120 revealed mixed levels of anti-CD4bs NAbs. Plasma BB12 contained CD4bs NAbs that were effective against the tier 1 virus HXB2 but not against the other viruses tested, including subtype C viruses (Fig. 3). It is possible that subtype C plasmas contain CD4bs Abs that are not adsorbed by the subtype B YU2 gp120. Further studies with subtype C gp120 will be required to address this point (Gray and Morris, unpublished data). As for plasma BB12, the CD4bs-neutralizing activity in plasmas BB14, BB81, and BB34 explained a substantial fraction of HXB2 virus neutralization and also accounted for some neutralization of primary subtype B and C viruses. However, in all cases, this was less than 50% of the total activity (Fig. 3).

Evaluation of CD4bs NAbs by native PAGE. BN-PAGE using native trimers may provide a way to evaluate NAbs directed to quaternary epitopes (22, 27) that may be difficult to detect by other methods. We previously used this assay to investigate monoclonal Fab, IgG, and polyclonal sera binding to functional WT trimers (12–14, 42). BN-PAGE exploits the tendency of hydrophobic surfaces to associate with Coomassie dye that imparts a uniform negative charge that is proportional to the Stokes hydrodynamic radius. This allows separation under nondenaturing conditions determined largely by the molecular weight of the protein or protein complex. In previous studies, only NAbs, and not nonneutralizing NAbs, could bind to trimers, confirming the relationship of trimer binding and neutralization (12–14, 42) suggested previously by others (56).

For mapping purposes, we evaluated mutant versions of native JR-FL trimers that were designed to selectively eliminate neutralization epitopes (Fig. 4). The trimers were previously estimated to be approximately 420 kDa, and incrementally 2G12-liganded trimers were thus estimated at ~570 kDa, ~720 kDa, and ~870 kDa (Fig. 4). The D368R mutant eliminated b12 and sCD4 binding but not 2G12 trimer binding (Fig. 4, upper panels). Conversely, mutant N295A eliminated 2G12 binding but not b12 or sCD4 binding (Fig. 4, upper panels). In the neutralization assays, these same patterns held true (Fig. 4, lower panels). However, the infectious counts of mutant viruses were lower than the infectious count of the WT parent, especially for the D368R mutant. Thus, in cases where a mutation renders trimers nonfunctional, BN-PAGE can help to discriminate binding from nonbinding. Importantly, the mutations did not have a globally disruptive effect on the trimers, as evidenced by their sensitivity to specificities not targeted by the mutations and resistance to nonneutralizing Abs in BN-PAGE (and the results of neutralization assays, where sufficient infectious counts allowed assessment).

We next sought to evaluate the plasmas. In these assays, our readout is a direct measure of plasma Ab binding to the same intact trimers as those used in the neutralization assays throughout this study. Furthermore, as unbound IgG is washed away before the trimers are isolated for native PAGE, any binding detected in this protocol is exclusively a reflection of Ab binding to spikes in situ on particle surfaces. Figure 5 provides a sample from a much larger data set in which trimer binding ID_{50}s were estimated by assessing the depletion of unliganded trimers by using densitometry. These were aver-

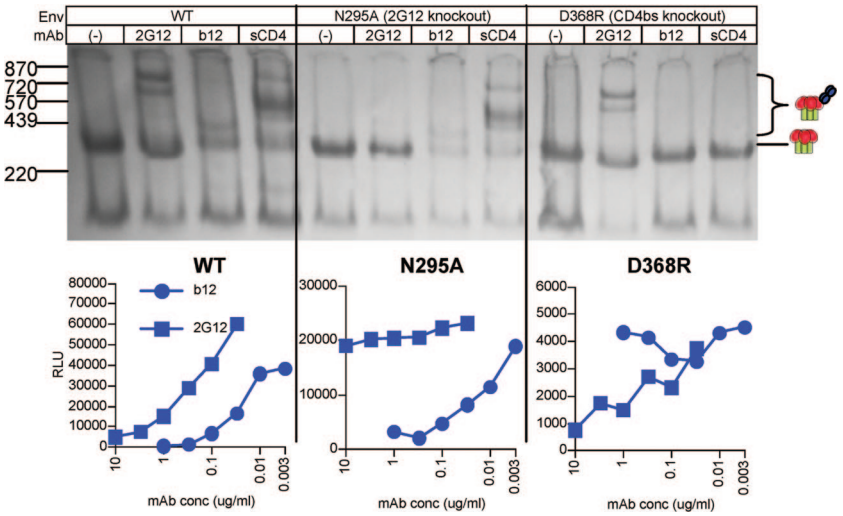

FIG. 4. Evaluation of WT and mutant JR-FL Envs in BN-PAGE and infectivity assays. Upper panel, WT, N295A (2G12 knockout mutant), and D368R (CD4bs knockout mutant) particles were incubated alone (−) or with one of the MAbs 2G12, IgG1b12, and sCD4 at 30 μg/ml. Trimers were then separated in BN-PAGE. Molecular mass markers for ferritin (220 and 439 kDa) and the estimated sizes of 2G12-liganded trimers (~570, ~720, and ~870 kDa) are indicated. Lower panel, WT and mutant particle sensitivities to neutralization by MAbs IgG1b12 and 2G12 were evaluated in neutralization assays with CF2 target cells. RLU, relative light units.

aged from at least two repeat titrations in addition to the data shown.

Initially focusing on the LT2 plasma, we observed strong binding to JR-FL WT trimers, with an ID_{50} of 1:500 (Fig. 5; data are summarized in Fig. 6), but relatively weak binding to the D368R trimer (Fig. 5, top panel), suggesting that approximately 98% of neutralizing activity was directed to CD4bs epitopes (Fig. 5 and 6). At high plasma concentrations, no WT

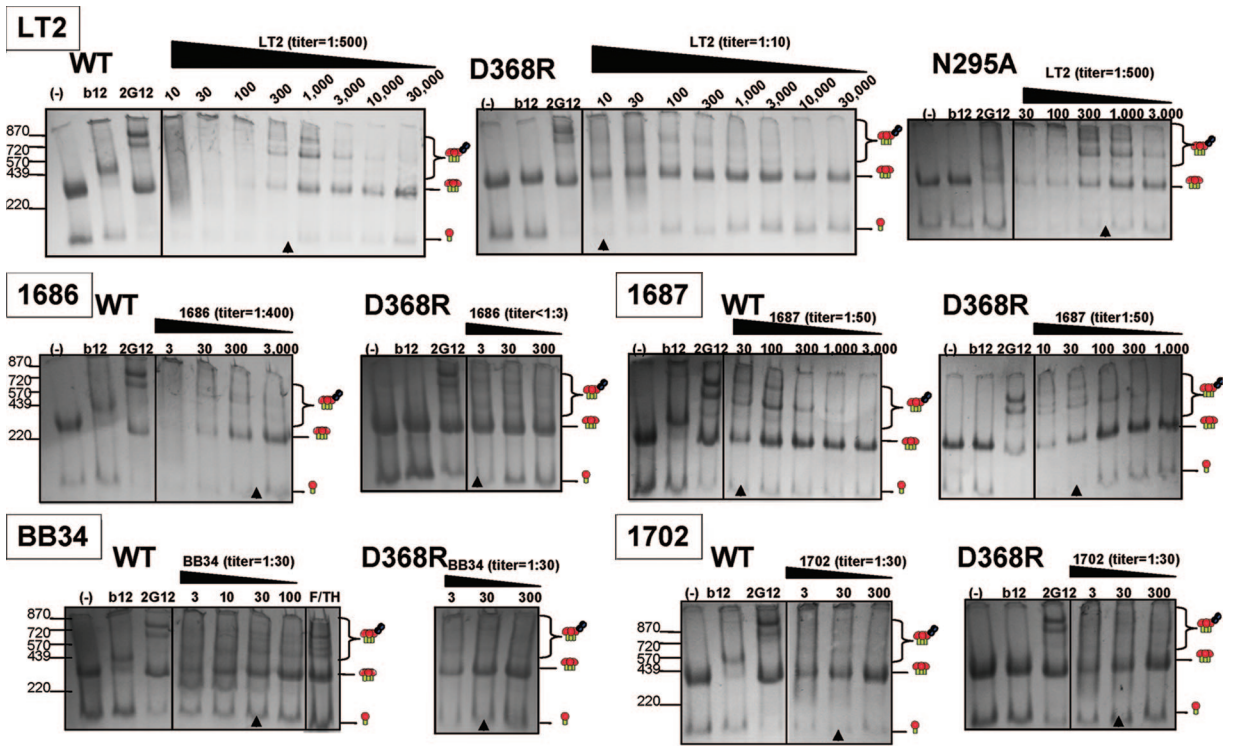

FIG. 5. Evaluation of plasma binding to WT and mutant trimers by BN-PAGE. Plasmas were titrated against WT, D368R, or N295A trimers in BN-PAGE as indicated. Cartoons depict gp120/gp41 trimers, trimer-IgG complexes, and monomers. Markers show the locations of ferritin markers of 220 and 439 kDa and trimers complexed with one, two, or three molecules of IgG 2G12 (molecular masses of ~570, ~720, and ~870 kDa). Arrows indicate the dilution corresponding to the ID_{50} titer, inferred from at least three duplicate titrations. The unbound fraction of plasma BB34 absorbed against WT gp120 beads was also evaluated for plasma BB34, identified as "F/TH," flowthrough. (−), blank beads.

plasma	JR-FL neut. ID50 titer	WT ID50 titer	D368R ID50 titer	% D368R sensitive	N295A ID50 titer	% N295A sensitive	2G12 capture titer
1648	40	3	<3	+	5	0%	20
1652	143	5	3	40%	5	0%	<20
1685	368	30	5	83%	30	0%	2,000
1686	1,329	400	<3	>99%	300	25%	<20
1687	911	50	50	0%	50	0%	600
1688	605	100	5	95%	100	0%	594
1702	192	30	30	0%	20	33%	<20
LT2	3,609	500	10	98%	500	0%	1,329
BB8	131	5	10	0	10	0%	<20
BB12	413	50	20	60%	30	40%	<20
BB14	40	10	<3	>70%	10	0%	<20
BB21	35	5	5	0%	5	0%	890
BB24	20	10	3	67%	10	0%	<20
BB28	35	20	3	85%	20	0%	<20
BB34	292	30	30	0%	30	0%	<20
BB47	100	10	30	0%	30	0%	<20
BB55	100	10	10	0%	10	0%	<20
BB68	<20	<3	3	N/A	n.d.	n.d.	N/A
BB75	150	5	5	0%	3	40%	<20
BB80	50	3	3	0%	3	0%	<20
BB81	80	10	10	0%	20	0%	<20
BB87	600	50	50	0%	100	0%	440
BB105	70	10	10	0%	10	0%	<20
BB107	600	100	50	50%	100	0%	<20
210	<20	<3	<3	N/A	<3	N/A	<20
211	<20	<3	<3	N/A	<3	N/A	<20

FIG. 6. Summary of results of mapping by native PAGE. Color coding is exactly as described in the Fig. 1 legend. ID_{50} neutralization (neut.) titers against JR-FL measured in the CF2 assay are indicated in the second column. ID_{50} titers of binding to WT, D368R, and N295A mutant titers are shown in the third, fourth, and sixth columns, respectively. The percentage of D368R (CD4bs)- or N295A (2G12-like)-sensitive activity was calculated with reference to the total activity against WT trimers (fifth and seventh columns). Gray-shaded cells in the fifth and seventh columns are considered significant, i.e., the titers differ by more than twofold, leading to a 50% or greater contribution to neutralization. ID_{50} competition titers for virus capture by the 2G12 MAb are shown in the eighth column. n.d., not done; N/A, not applicable.

trimer complexes were visible (Fig. 5), a result reminiscent of those of our previous BN-PAGE experiments using IgGs b12 and 2F5 (12). However, at dilutions close to the ID_{50}, liganded trimer complexes became visible. The most prominent of these appeared to correspond to a trimer complexed with two IgG molecules (12). However, detailed inferences on the nature of the trimer complexes are precluded by the possibility that plasma NAbs may consist of more than one IgG specificity bound simultaneously to trimers and, possibly, even neutralizing IgA that would be expected to migrate differently than IgG.

Similar analyses were performed with the other subtype B plasmas, and representative blots are shown in Fig. 5. All but the 1687 and 1702 plasmas bound the WT trimer more efficiently than the D368R mutant (Fig. 5; data are summarized in Fig. 6). The contribution of CD4bs activity was high in plasmas LT2, 1686, and 1688 that neutralized JR-FL very effectively (ID_{50}, >1:500), consistent with previous observations that the JR-FL isolate is unusually sensitive to b12 and that these plasmas contain b12-like NAbs (5) (Fig. 1 and data not shown). The trimer binding ID_{50} titers of the seven commercial subtype B plasmas were lower than that of LT2, consistent with their somewhat lower neutralization titers. However, binding was still readily observable (Fig. 5) and quantifiable by densitometry.

As for plasma LT2, IgG-liganded WT trimer complexes with other subtype B plasmas tended to resolve only at higher dilutions (Fig. 5 and data not shown). In some cases, three or more trimer complex bands were observed, suggesting various complexes. Plasmas 1685, 1686, 1687, and 1688 formed complexes of similar size that might be best approximated as trimers complexed with two IgG molecules, similar to those observed with plasma LT2 (Fig. 5 and data not shown). However, the other three subtype B plasmas exhibited either no visible complexes (1702) or other patterns (1648 and 1652) (Fig. 5 and data not shown). Although it is not yet clear what these complexes represent, it seems worth suggesting the possibility that neutralization may be achieved by a conserved mechanism in cases that exhibit similar patterns in this assay.

A similar analysis of subtype C plasmas revealed much less sensitivity to the D368R mutation than were found for the subtype B plasmas (Fig. 5 and 6). In many cases, titers against the D368R mutant were identical to those against the parental trimers. Only 5 of 15 subtype C plasmas with measurable binding to JR-FL trimers (excluding plasma BB68 which failed to neutralize JR-FL effectively) contained detectable D368R sensitivity, in contrast to 6 of 8 subtype B plasmas. Furthermore, none were >90% sensitive to the D368R mutant. Plasma BB34 exhibited equivalent binding to both WT and mutant gp120 (Fig. 5 and 6), implying a lack of CD4bs activity, in keeping with the gp120 adsorption results (Fig. 3). Faint trimer complexes were observed (Fig. 5, bottom left). IgG derived from the unbound ("flowthrough") fraction from WT gp120 adsorption of plasma BB34 was also examined. Here, the trimer complex bands were as well resolved as with the unfractionated plasma (Fig. 5, bottom left). The fact that little or no trimer binding activity was lost after gp120 adsorption is consistent with the idea that a significant fraction of the neutralizing activity of this plasma derives from non-gp120 binding NAbs, perhaps directed to gp41.

A comparison of WT trimer binding ID_{50}s and neutralizing ID_{50}s of all 24 plasmas (Fig. 6, second and third columns) revealed a good correlation (Pearson correlation coefficient, 0.922 [$P = 1.63 \times 10^{-10}$], and Spearman rank correlation coefficient, 0.808 [$P = 1.82 \times 10^{-6}$]). Furthermore, the neutralization ID_{50}s were consistently stronger than the trimer ID_{50}s, although the difference was somewhat variable. For all 24 plasmas, the difference was ~11-fold (standard deviation, 7.9-fold). There were no significant differences when subtype B or C plasmas were considered separately. Clearly, neutralization begins at plasma concentrations lower than those at which we observe significant depletion of trimer in gels. The results of a previous analysis revealed that certain MAbs (b12 and 2F5) neutralize JR-FL up to 100-fold more potently than they bind to trimers (12), but others bind trimers and neutralize with similar IC_{50}s (2G12, 4E10, and Z13e1). Thus, it appears possible that NAbs with specificities similar to those of b12 or 2F5 might contribute to the neutralizing activities of our plasmas.

A comparison of the data from the six plasmas with useable CD4bs data in each of our two assays (Fig. 3 and 6) revealed only weak conformity (Pearson correlation coefficient, 0.615 [$P = 0.193$], and Spearman rank correlation coefficient, 0.551 [$P = 0.257$]). High levels of D368R-sensitive NAbs were detected in plasmas 1686 and BB14 in both assays. Plasma 1652 exhibited a modest level of CD4bs-directed NAbs in both assays. Weak or no D368R-mutant-sensitive activity against JR-FL was detected in both assays by plasmas BB34 and BB81. Although plasma BB12 was intermediately sensitive to the D368R mutant in BN-PAGE, this activity was not detected in gp120 adsorptions against JR-FL, but it was detected against several other viruses (Fig. 3). This was the main outlier point that reduced the significance of the correlation coefficients (the

other, less-significant outlier was plasma BB81). One possible explanation for the discrepancy is that the D368R mutation of monomeric gp120 and trimers may have slightly different consequences for NAb binding. In addition, the use of mismatched Envs (YU2 and JR-FL) in these two methods might also have contributed to the somewhat-different outcomes. The discrepancy is, however, unlikely to be a native PAGE artifact, since, as mentioned above, the protocol exclusively measures binding to intact trimers in situ on particle membranes, so the results can be directly cross-referenced with neutralization data.

Mapping of 2G12-like Abs by native PAGE and virus capture competition. MAb 2G12 does not compete with any other known MAbs directed to gp120 or gp41 (41). Therefore, competitive binding assays may be useful in assessing 2G12-like activity, even when the readout is not associated with neutralization (7, 17). In competitive virus capture assays on 2G12-coated plates, some of the subtype B plasmas (1648, 1686, 1687, 1702, and LT2) and two of the subtype C samples (BB21 and BB87) were found to inhibit virus capture (Fig. 6) but control HIV-negative plasmas were not (not shown).

Another way to examine 2G12-like Abs is by BN-PAGE shift assays using N295A mutant trimers. In many cases, including plasma LT2, the titers against the 295 mutant were very similar to those against the WT parent (Fig. 5 and 6), suggesting that few, if any, 2G12-like NAbs were present, even in those plasmas that competed with 2G12 in virus capture (Fig. 5 and 6). Overall, these results suggest that a fraction of patients develop binding Abs that overlap the 2G12 epitope, but unlike 2G12, these Abs tend not to neutralize the virus (7).

Analysis of gp41-directed neutralizing activity. We next investigated gp41 MPER-neutralizing activity (54, 62, 71) using three assays: (i) a post-CD4/CCR5 neutralization assay (3, 14), (ii) a neutralization assay using HIV-2 scaffolds bearing various MPER epitope motifs, and (iii) peptide interference neutralization assays. MPER data from all three assays is summarized in Fig. 7.

The post-CD4/CCR5 assay measures neutralizing activity against epitopes that remain available after trimer engagement with both CD4 and CCR5. So far our tests have shown that only MPER NAbs mediate significant neutralization in this format (Fig. 7) (3, 14). However, we cannot rule out possible neutralization by other gp41-specific or even gp120-specific Abs. Using known MPER NAbs, we first evaluated the relative sensitivities of the post-CD4/CCR5 and standard formats. MAbs 2F5 and 4E10 neutralize equivalently in both formats, while MAb Z13e1 neutralizes about fourfold more potently in the post-CD4/CCR5 format (Fig. 7, second and third columns). Given these roughly equivalent assay sensitivities, we can therefore estimate the percent contribution of MPER NAbs to overall neutralization titers. As reported previously, IgG1b12 did not neutralize in the post-CD4/CCR5 format (14).

Weak post-CD4/CCR5 neutralization was detected in five of the eight subtype B plasmas (1648, 1652, 1688, 1702, and LT2) (Fig. 7). Comparing these titers to those in the standard format, taking plasma 1648 as an example, an ID_{50} titer of 1:40 in the standard assay and 1:8 in the post-CD4/CCR5 assay indicates that an estimated 20% of total neutralization activity is directed to the MPER (Fig. 7, fourth column). Remarkably, the subtype C plasma BB34 exhibited a very strong post-CD4/CCR5 titer of 1:200 that constituted most (~69%) of its neutralizing activity, as measured in the standard format. BB81 and BB105 were the only other subtype C plasmas in our panel with detectable MPER reactivity, albeit with extremely low titers.

plasma	JR-FL neutralization: standard	JR-FL neutralization: post-CD4/CCR5	JR-FL neutralization: % MPER	HIV-2/YU2 C1 chimera neutralization
1648	40	8	20	1,044
1652	143	19	13	884
1685	368	<2	<1	225
1686	1,329	<2	<1	55
1687	911	<2	<1	73
1688	605	3	1	78
1702	192	31	16	641
LT2	3,609	28	8	<20
BB8	131	<2	<2	31
BB12	413	<2	<1	46
BB14	40	<2	<5	32
BB21	35	<2	<6	35
BB24	20	<2	<10	170
BB28	35	<2	<6	353
BB34	292	200	69	6,734
BB47	100	<2	<2	453
BB55	100	<2	<2	42
BB68	<20	<2	<10	124
BB75	150	<2	<1	83
BB80	50	<2	<4	31
BB81	80	5	6	326
BB87	600	<2	<1	70
BB105	70	3	4	62
BB107	600	<2	<1	20
210	<20	<2	N/A	
211	<20	<2	N/A	
2F5	0.2	0.3		0.138
4E10	2	3		0.0731
Z13e1	26	6		0.282
IgG1b12	0.04	>30		N/A

FIG. 7. Summary of MPER-neutralizing activity. MPER ID_{50} titers were measured in post-CD4/CCR5 and HIV-2 MPER graft neutralization assays. Post-CD4/CCR5 activity (third column) is expressed as a percentage, given to the nearest integer (fourth column), of that in the standard format (second column), both assayed on CF2 cells. Titers against the YU2 C1 MPER/HIV-2 chimera virus (fifth column) have been adjusted to subtract the HIV-2 7312A background titers (Fig. 1), so that all the activity is likely to be directed against the MPER. The IC_{50}s of MPER MAbs 2F5, 4E10, and Z13e1 were also determined in each assay, expressed in μg/ml. Boxes have color coding similar to that in Fig. 1; gray-shaded boxes in the fourth column indicate samples with significant MPER activity. N/A, not applicable.

We next evaluated the plasma activities against scaffold pseudoviruses with subtype B (YU2) MPER fragments grafted into the equivalent site of an HIV-2 Env. The sequences of the parental chimera, C1, and several derivatives, C3, C4, C4GW, C6, C7, and C8, are depicted in Fig. S3 in the supplemental material. These were designed to preferentially expose particular segments of the MPER domain to gain insight into the fine specificities of MPER Abs. A comparison of the MAb titers in this assay and in the standard format (Fig. 7, bottom of second and fifth columns) revealed that MAbs 4E10 and Z13 are particularly potent against the YU2 chimera, while the 2F5 titers for the two were similar. One possible explanation is that the YU2 and JR-FL MPER regions exhibit inherently different susceptibilities to these MAbs. Alternatively, the exposure of various MPER epitopes may be differentially affected by their context in Env scaffolds.

A comparison of plasma ID_{50}s in the post-CD4/CCR5 and C1 chimera neutralization assays (Fig. 7, third and fifth columns) revealed the latter to be far more sensitive, with a mean titer difference between the two assays of 91-fold but considerable variation in the differences (standard deviation, 110.4), assuming that all values of <2 are taken as 1. This discrepancy may stem at least in part from slightly different inherent susceptibilities of the two Envs to MAbs similar to 4E10 and

Z13e1, as discussed above. Nevertheless, some weak conformity was observed between the results of the two assays, as judged by a Kendall's rank correlation of 0.36 ($P = 0.026$) and a Spearman's rank correlation of 0.44 ($P = 0.031$) (in which all values of <2 were ranked equally). The C1 chimera neutralization titers were particularly strong with plasmas 1648, 1652, 1702, and BB34 (all ID_{50}s were >1:500), all of which also had detectable activity in the post-CD4/CCR5 assay. However, MPER activity against the C1 chimera was undetectable in plasma LT2, consistent with the results of a previous report using the same assay (18) but inconsistent with the low but nevertheless detectable MPER activity in the post-CD4/CCR5 assay. It is possible that the activity in this plasma is directed against an N-terminal MPER epitope like 2F5 that is detected relatively inefficiently by the C1 chimeras.

We next inspected the activities of the subtype B plasmas against the various MPER-engrafted mutant viruses (depicted in Fig. S3 in the supplemental material) with reference to the activities of MPER MAbs 2F5, 4E10, and Z13e1. The results of this analysis are shown in Fig. S4 in the supplemental material. Each MAb prototype exhibited a different pattern of activity against this panel of chimeras. MAb 2F5 neutralized the C3 and C7 chimeras; 4E10 neutralized the C4, C4GW, C6, and C8 chimeras; and Z13e1 neutralized only the C4GW and C8 chimeras. The subtype B plasmas exhibited various neutralization patterns that in no case exactly recapitulated those of any one of the prototypes. This may suggest the coexistence of multiple known MPER specificities and/or new specificities unlike any of the prototype MAbs. Despite the overall complexity of the plasma MPER responses, the potent activities of plasmas 1648 and 1702 against the C4GW mutant suggest Z13-like NAbs, whereas the activity of 1652 against C4 and C6 suggests 4E10-like NAbs. We did not address the fine mapping of the subtype C plasmas here, as this will form part of a separate study (Gray and Morris, unpublished).

We further assessed MPER activity in neutralization interference assays using the peptides depicted in Fig. S3 in the supplemental material. The full analysis is shown in Fig. S5, and essential data are summarized in the 10th column of Fig. S4, both of which are in the supplemental material. The MPR.03 peptide covers the entire MPER domain, and the HXB2.2F5.01 and 4E10.22 peptides cover 2F5- and 4E10-like specificities, respectively (see Fig. S3 in the supplemental material). Peptides designed for Z13e1 adsorption markedly affected virus infection and were therefore not investigated further. We first validated the peptides using known MPER MAbs. MPR.03 effectively blocked the neutralizing activities of 2F5, 4E10, and Z13e1 against the 7312A C1 chimeric virus, demonstrating its ability to capture all known MPER Abs. The 4E10.22 peptide blocked 4E10 and Z13e1 but not 2F5 neutralization, whereas the HXB2 2F5.01 peptide inhibited 2F5 but not 4E10 or Z13e1 neutralization (see Fig. S5 in the supplemental material).

Having established the peptide specificities, we next assessed their effects, if any, on subtype B plasma neutralization. The data are shown in Fig. S5 in the supplemental material; twofold or greater changes in ID_{50} indicate that more than one-half of the NAb titer was blocked. For all four plasmas, competition with the MPR.03 peptide reduced JR-FL neutralization by twofold or less (Fig. S5 in the supplemental material), consistent with their relatively weak or absent activity in post-CD4/CCR5 assays (Fig. 7, third column) in proportion to the total neutralization activity in each case.

We next assessed peptide interference in neutralization assays with the MPER-grafted HIV-2 7312A C1 chimera that should only be susceptible to MPER-directed NAbs. Neutralization by all four plasmas was substantially inhibited by the MPR.03 and 4E10 peptides but not by the 2F5 peptide (see Fig. S5 in the supplemental material; data are summarized in Fig. S4, 10th column, in the supplemental material), confirming the presence of Z13e1 and/or 4E10-like Abs. This was consistent with the strong activity detected with three out of four of these plasmas against the C8 chimera, which encompasses a 3′ part of the MPER region similar to the 4E10.22 peptide and can detect 4E10- and Z13-like activity. The exception was plasma 1686, which had somewhat lower but detectable anti-C8 activity that could conceivably contribute to the C1 mutant neutralization observed in the peptide interference assays in this study.

Peptide interference of HXB2 neutralization was weaker and only reached significance for plasma 1686. This may reflect the sensitivity of HXB2 to neutralization by specificities that do not recognize the 7312A chimera, thereby emasculating the potency of MPER peptides in neutralization interference.

Summarizing the results for MPER activities, we detected low titers of post-CD4/CCR5 NAbs against JR-FL in almost all cases, the specificities of which appeared to be quite complex and variable. The results of peptide interference assays suggested the presence of Z13- or 4E10-like rather than 2F5-like activity in four of the subtype B plasmas.

Neutralizing activity directed against the V3 loop. There are reasonable arguments for and against a role for V3 Abs in broad plasma neutralization. While the V3 loop is largely occluded on primary isolate trimers such that V3 Abs tend to neutralize primary isolates rather weakly (6), the high titers of V3 Abs often observed in natural infection could conceivably factor into overall neutralization titers (40). Furthermore, although V3 loop Abs are classically considered to be highly strain specific, certain V3 Abs react with more conserved elements and, therefore, may in some cases be capable of cross-neutralizing activity (45, 70).

Three approaches were used to measure V3 loop activity in our plasma panel. One was to measure the abilities of plasmas to inhibit the capture of JR-FL virus particles by a V3 MAb, 39F. Subtype B plasmas exhibited modest titers in this assay (Fig. 8, third column) and lower activities were found in the subtype C plasmas, suggesting subtype-specific V3 loop binding. A caveat regarding this assay is that capture may be blocked by non-V3 specificities, as well as V3 Abs. Therefore, in a second assay, we evaluated V3 reactivity using a chimeric HIV-2 virus engrafted with the HIV-1 YU2 or subtype C consensus V3 loop in place of the equivalent parental sequence (see Fig. S6 in the supplemental material) (Davis et al., submitted). High titers of V3 loop Abs were observed in most cases (Fig. 8, fourth and fifth columns). The V3 reactivity was again found to be somewhat subtype restricted, so that plasmas better neutralized the matched chimera, as reflected by the behavior of subtype B patient-derived MAbs 447-52D and F425. However, the subtype C plasmas showed higher overall V3 reactivity in this assay, in many cases giving higher titers

plasma	JR-FL neutralization	virus capture anti-V3 loop mAb 39F	HIV-2 V3 chimeras HIV-2 KR YU2 V3 loop	HIV-2 KR Ccon V3 loop	peptide interference JR-FL V3.01	JR-FL V3.02	JR-FL d.301 V3.01	JR-FL d.301 V3.02	TV1 V3.01	TV1 V3.02	MW965 V3.01	MW965 V3.02
1648	50	1,270	4,739	687	1.1	1.5	1.9	0.8	1.1	>11.9	1.1	1.2
1652	100	600	<500	<500	0.9	1.1	1.3	1.0	1.1	>6.2	0.8	0.9
1685	364	4,880	n.d.	n.d.	0.9	0.7	1.1	0.8	n.d.	n.d.	n.d.	n.d.
1686	776	1,656	2,725	1,684	0.9	1.5	1.3	0.9	1.6	>4.6	n.d.	0.8
1687	1,957	1,427	n.d.	n.d.	1.2	1.1	1.2	1.0	n.d.	n.d.	n.d.	n.d.
1688	732	3,000	n.d.	n.d.	0.9	0.9	1.4	1.1	n.d.	n.d.	n.d.	n.d.
1702	192	4,880	1,495	1,684	1.5	1.3	5.5	1.2	1.5	5.5	0.8	0.9
LT2	3,609	4,328	n.d.	n.d.	1.2	0.9	n.d.	n.d.	n.d.	n.d.	n.d.	n.d.
		447-52D	0.0013	0.0335	8.3	0.6	>208	0.9				
		F425	0.007	0.7095								

plasma	JR-FL neutralization	virus capture anti-V3 loop mAb 39F	HIV-2 V3 chimeras HIV-2 KR YU2 V3 loop	HIV-2 KR Ccon V3 loop	peptide interference JR-FL V3.01	JR-FL V3.02	JR-FL d.301 V3.01	JR-FL d.301 V3.02	TV1 V3.01	TV1 V3.02	MW965 V3.01	MW965 V3.02	ZA01 V3.01+V3.02
BB8	131	560	2,475	2,000	0.8	0.4	0.9	0.7	0.9	0.4	1.2	n.d.	n.d.
BB12	413	<20	1,613	2,534	0.9	0.7	0.7	0.8	1.3	2.5	1.8	n.d.	n.d.
BB14	40	811	10,425	13,516	n.d.	n.d.	n.d.	n.d.	1.6	0.9	1.8	0.9	n.d.
BB21	35	2,500	4,617	55,426	n.d.	n.d.	n.d.	n.d.	3.6	0.7	12.5	0.8	n.d.
BB24	20	920	1,525	20,082	n.d.	n.d.	n.d.	n.d.	2.4	1.7	23.9	0.7	n.d.
BB28	35	<20	989	11,789	n.d.	n.d.	n.d.	n.d.	1.9	0.4	8.3	0.9	1.2
BB34	292	1,500	35,138	24,647	1.4	0.8	n.d.	n.d.	2.8	0.9	7.7	0.9	1.4
BB47	100	<20	62	6,393	0.8	0.7	n.d.	n.d.	1.2	0.3	1.6	n.d.	n.d.
BB55	100	<20	1,830	10,353	0.9	0.5	0.9	0.7	4.4	1.5	3.9	0.8	n.d.
BB68	<20	500	746	3,193	n.d.	n.d.	n.d.	n.d.	2.5	4.6	n.d.	n.d.	1.1
BB75	150	990	10,538	9,698	0.4	0.1	1.3	1.8	2.0	5.9	n.d.	n.d.	1.3
BB80	50	960	2,831	4,654	n.d.	n.d.	n.d.	n.d.	n.d.	n.d.	n.d.	n.d.	n.d.
BB81	80	<20	127	2,101	0.9	1	0.9	0.7	1.5	3.7	n.d.	n.d.	n.d.
BB87	600	250	2,858	30,927	0.5	0.7	1.1	0.9	2.4	1.1	n.d.	n.d.	n.d.
BB105	70	850	6,872	8,366	1.0	1.1	1.7	0.8	4.6	4.8	4.2	1.0	0.8
BB107	600	1,100	2,242	5,401	0.9	0.9	1.6	0.9	n.d.	n.d.	79.1	5.5	n.d.
							WGP 102-4		5.6	1.8	49.4	1.1	

FIG. 8. Summary of V3 activity. V3 activity was measured by (i) competition of virus capture by a V3 MAb 39F (third column), (ii) neutralization of the HIV-2 KR virus engrafted with either the YU2 or a consensus subtype C V3 loop (fourth and fifth columns), and (iii) by peptide interference assays (6th to 14th columns). Virus capture and chimera neutralization data are given as ID_{50} titers. Peptide interference was recorded as the severalfold change in ID_{50} titer with reference to the titer of controls to which no peptide was added. Virus capture and chimera neutralization assay data are color coded as described in the Fig. 1 legend. Boxes depicting the results of peptide interference experiments in which significant competition was observed (more-than-twofold effect) are shaded gray; results indicating no significant competition (less-than-twofold effect) are unshaded. Controls included V3 MAbs 447-52D, F425, and guinea pig serum WGP 102-4 (66). n.d., not done.

than the subtype B plasmas against the subtype B chimera. This finding contrasted with the relatively weak ability of subtype C plasmas to block the capture of the subtype B isolate JR-FL by a V3 MAb. The underlying reason for this discrepancy is not clear but could be related to the different contexts in which the V3 sequences are presented (Fig. 8, compare bottom and top halves of third and fourth columns).

A caveat regarding this second assay is that the chimeras are acutely sensitive to the V3 MAbs 447-52D and F425 from subtype B donors (Fig. 8). Therefore, in a third approach to investigate the significance of the V3 activity, we evaluated the abilities of V3 peptides to interfere with the neutralization of several HIV-1 isolates, including several primary isolates (Fig. 8, 6th to 14th columns). Two types of V3 peptides were synthesized, matching each virus (see Fig. S6 in the supplemental material). The V3.01 series were derived from the N-terminal part of the loop, including the crown, and the V3.02 series were derived from the C-terminal part of the loop. Using MAb 447-52D and the V3-sensitive d.301 derivative of JR-FL, we found that the V3.01 peptide potently inhibited neutralization but the V3.02 peptide had no effect. The V3.01 peptide also blocked BaL.26 and SF162.LS neutralization by a panel of six other V3 MAbs (data not shown), indicating that V3 Abs are commonly directed to the N-terminal part of the V3 loop. In the examination of the subtype B plasmas, neither peptide convincingly interfered with WT JR-FL neutralization (changes of less than twofold) (Fig. 8), consistent with the general V3 resistance of this primary isolate. However, the V3.01 peptide strongly inhibited neutralization by plasma 1702 against d.301 JR-FL (a 5.5-fold decrease in ID_{50} titer) and had some effect (1.9-fold) on plasma 1648. A twofold effect on the ID_{50} titer indicates that 50% of virus neutralization can be assigned to the V3 loop. JR-FL d.301 neutralization by the remaining subtype B plasmas was not significantly affected by V3 peptides.

We next evaluated V3 peptide interference against the subtype C virus TV1. TV1 is comparable to JR-FL in terms of overall neutralization sensitivity (Fig. 1), but the results of previous studies have indicated that it is partially sensitive to V3 neutralization (66). In contrast to JR-FL d.301, the V3.02 peptide rather than the V3.01 peptide blocked a substantial portion of subtype B plasma neutralization against TV1 (Fig. 8 and 9). Therefore, cross-subtype Abs targeted to the C-terminal portion of the V3 loop contributed markedly to TV1 neutralization. Thus, for plasma 1686, the highly potent CD4bs activity found to be effective against JR-FL was relatively ineffective against TV1 (1:22 for TV1 versus 1:1,329 for JR-FL) (Fig. 1), which instead appears to be neutralized in large part by NAbs directed to the C-terminal portion of the V3 loop. In contrast to TV1, neutralization of the sensitive MW956 subtype C isolate could not be inhibited by either peptide (Fig. 8). This is probably because MW965 is highly sensitive to most known MAbs, and non-V3 specificities may therefore dictate the neutralization of this tier 1 isolate.

We next investigated V3 peptide interference in neutralization by the subtype C plasmas. V3 peptides were unable to interfere with either JR-FL or its sensitive d.301 derivative, suggesting that cross-subtype neutralization of these isolates is not mediated by V3-specific NAbs. As with the subtype B plasmas, TV1 neutralization by subtype C plasmas was sensitive to adsorption by V3 peptides. Here, however, either or both of the peptides V3.01 and V3.02 were effective, as exemplified by the results for plasmas BB21 and BB68 shown in Fig. 9. Therefore, neutralization was not restricted to the V3 C terminus as with the subtype B plasmas (Fig. 8). In contrast, neutralization of the MW956 isolate was blocked by the V3.01

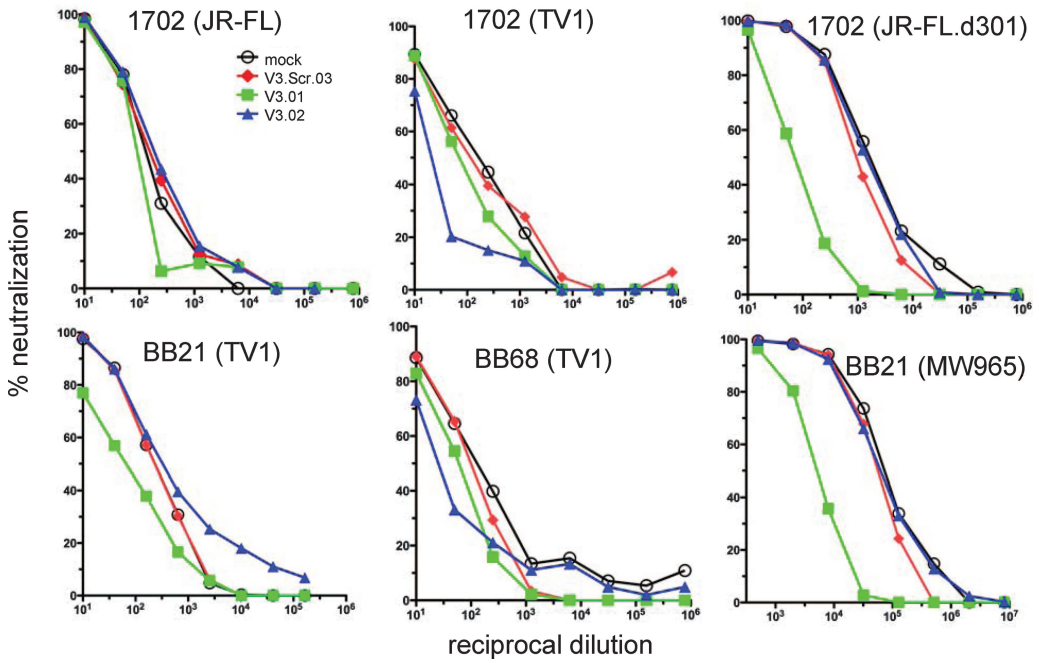

FIG. 9. Roles of the V3 N and C termini in subtype B and C neutralization. Viruses and plasmas were incubated in the presence or absence of 25 μg/ml of the interfering peptide indicated, and neutralization was subsequently measured using the TZM-bl assay. In each experiment, V3 peptides (depicted in Fig. S6 in the supplemental material) were matched to the sequence of the virus used in neutralization assays. The "V3 Scr.03" peptide was included as an assay control. Its sequence, NKGTHNIPTARNIYGFPTSRRGT, is based on jumbled V3 residues.

peptide only, reminiscent of the activities of some subtype B plasmas against JR-FL d.301 (Fig. 8 and 9). Hence, the subtype C plasmas neutralize TV1 by epitopes on either side of the V3 crown, but neutralization of the sensitive subtype C isolate appears to be restricted to the V3 N terminus, analogous to subtype B plasma neutralization of JR-FL d.301. As an additional control, a guinea pig vaccine antiserum with a high V3 titer against a subtype A V3 (66) was assayed against these two subtype C isolates. In each case, neutralizing activity was adsorbed by the V3.01, not the V3.02 peptide (Fig. 8). We also examined V3 interference of neutralization against another subtype C primary isolate, ZA12, known to be generally resistant to V3 neutralization. There, akin to the results for JR-FL, the V3 peptides had little or no effect (Fig. 8).

Activity directed to the CD4i epitope of gp120. The chemokine receptor binding domain (closely related to the CD4i epitope) of gp120, like the V3 loop, is largely occluded on primary isolate trimers and, as a result, neutralization via this specificity is usually modest and sporadic. Nevertheless, it is possible that extremely high titers of CD4i Abs, as often found in chronic HIV+ infection (16), can contribute to overall neutralization titers. We evaluated CD4i titers in two assays. First, we assessed the abilities of plasmas to inhibit virus capture by the CD4i MAb E51 in the presence of sCD4, to increase epitope exposure. Titers were high in every case, and did not differ significantly between the subtype B and C plasmas (Wilcoxon 2 sample test [$P = 0.481$]) (see Fig. S7 in the supplemental material). In a second assay, we measured neutralization against an HIV-2 isolate in the presence of sCD4. Given the conservation of the CD4i epitope, CD4i MAbs are able to cross-neutralize HIV-2 in this format (16). The titers were generally lower than those in the first assay (see Fig. S7 in the supplemental material), barring a few exceptions, and did not correlate well with the virus capture data (Pearson coefficient, 0.191 [$P = 0.37$]), which could be explained by any of the numerous qualitative differences between these two assays. For example, CD4bs, as well as CD4i, Abs can inhibit E51 capture, artificially increasing titers (J. M. Binley and E. T. Crooks, data not shown). In addition, despite the considerable conservation of this epitope between HIV-1 and HIV-2, HIV-2 viruses conceivably may not capture all HIV-1-directed CD4i activity. Overall, however, since neither assay effectively measures neutralizing CD4i activity against primary viruses, we do not know the significance of these titers relative to JR-FL neutralization. However, given the limited ability of CD4i MAbs to neutralize JR-FL, we expect the contribution is minimal, as for V3 Abs.

Summary of neutralizing activities. Estimates of the proportional contributions of different Ab specificities to the total JR-FL gp160ΔCT neutralization titers are shown in Fig. 10. The CD4bs activity was estimated from the results of trimer shift assays (Fig. 6), and MPER activity was estimated from post-CD4/CCR5 neutralization data (Fig. 7). The percentages of gp120-directed activity from the data shown in Fig. 3 are also given where available. Overall, the results shown in these pie charts indicate that CD4bs NAbs contribute a large proportion of the JR-FL-neutralizing activity in half of the subtype B plasmas. Relatively minor MPER activity was detected in five of the eight subtype B plasmas. In comparison, the subtype C plasmas contained generally less CD4bs activity (5/16 plasmas) and less MPER activity (3/16 plasmas).

We selected JR-FL as our prototype for mapping here be-

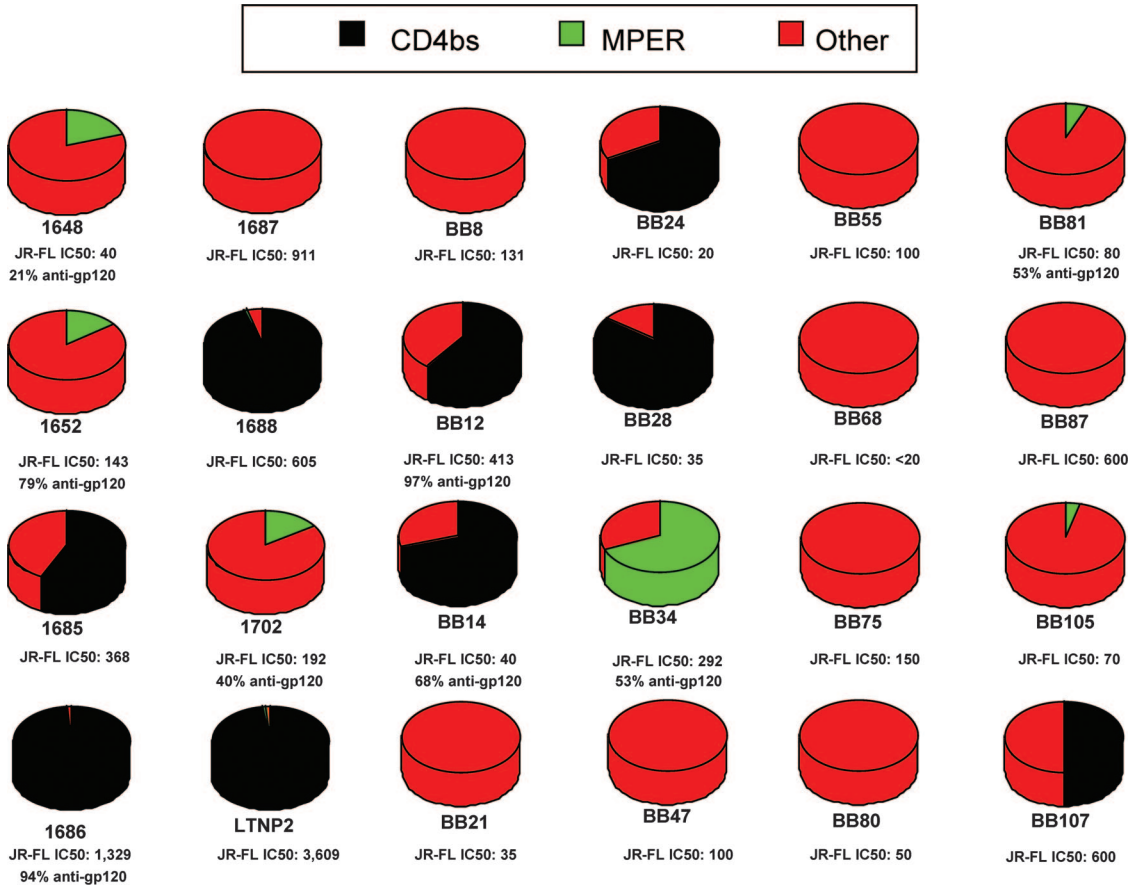

FIG. 10. Summary of estimated contributions of plasma specificities involved in JR-FL neutralization. CD4bs activities are derived from the trimer shift data shown in Fig. 6, and MPER activities are derived from the post-CD4/CCR5 activities shown in Fig. 7. Any remaining activities unaccounted for by mapping are depicted as "other." Due to uncertainty regarding activity that is <50% of the total in native PAGE and peptide interference assays (Fig. 8), we only include data showing a >50% contribution to total neutralization, thus eliminating possible minor contributions by V3- and 2G12-like NAbs in these pie charts. The percentages of gp120-specific neutralization are derived from the data shown in Fig. 3.

cause of its wide historical use as a common primary isolate in the field. We acknowledge that the specificities by which plasmas neutralize the JR-FL isolate may differ from those that neutralize other primary subtype B isolates or other subtypes, as suggested by the adsorption data in Fig. 3. For example, the CD4bs NAbs of plasma 1686 contribute significantly but variously to the neutralization of primary isolates, but not at all against tier 1 isolates; neither does this plasma effectively neutralize the subtype C isolate TV1, which instead appears to be neutralized (if rather weakly) by V3 Abs. It is also possible that the subtype C plasmas contain NAbs directed to subtype-specific targets that are not available on subtype B Envs. However, the overriding finding from the present analysis is that about two-thirds of the activity of subtype B and subtype C plasmas that is responsible for neutralizing the JR-FL subtype B virus could not be mapped by any of our assays, suggesting the presence of NAbs with specificities unlike any of the few known broadly neutralizing prototype MAbs.

It is worth mentioning some caveats. Our methods were all focused on neutralization assays performed in immortalized cell lines. This facilitates the consistent measurement of neutralization titers that is important for many of our mapping methods. On the other hand, PBMC-based neutralization assays are generally considered to be more physiologically relevant. Since MPER NAbs, and in particular 4E10-like Abs, are known to perform relatively poorly in PBMC assays, the MPER activity represented in Fig. 10 may be a slight overestimation (5, 63). Furthermore, we know from the results of previous studies that the truncated gp160 mutant virus is somewhat more sensitive to MPER NAbs than its full-length counterpart (14, 23), compounding the likelihood that the estimated proportions of MPER NAbs shown in Fig. 10 are modest overestimates. CD4i Ab results were omitted from Fig. 10 since we lack a definitive way to map this activity. Any possible minor contributions by 2G12 and V3 NAbs are not included, as the accuracy of our assays is such that we only considered greater-than-twofold effects to be significant. Finally, a possible confounding factor in our mapping efforts is that although NAbs may neutralize synergistically or antagonistically in polyclonal mixtures, these relationships are eliminated in assays where specificities or groups of specificities are assayed independently (e.g., gp120 fractionations and MPER assays), possibly skewing the measurement of titers.

Overall, we wish to emphasize that the proportions shown in

Fig. 10 are estimates influenced both by the accuracy of each assay (although most assays were repeated several times to ensure consistency) and by interassay protocol differences. A clear example of the limits of our estimates is the apparent contradiction that approximately 70% of the neutralizing activity of plasma BB34 apportioned to the gp41 MPER in the post-CD4/CCR5 assay but 53% was allocated to gp120 in adsorption experiments. We interpret this by suggesting that approximately half the activity against JR-FL is directed against MPER and half against gp120.

DISCUSSION

We attempted to define the basis of broad neutralization in a collection of subtype B and C HIV-1 plasmas. We intended to illuminate the relative importance of various known neutralizing epitopes as potential targets for vaccine development, as well as to provide insights into possible novel neutralizing epitopes. This is the largest and most-comprehensive data set of its kind to be generated to date. The results of the initial gp120 adsorption experiments (Fig. 2 and 3) revealed that gp120 activity accounts for a significant but variable fraction of the neutralization, depending on the virus isolate. For some plasmas, broad neutralization was mediated by anti-gp120 Abs, and in some cases, CD4bs-directed NAbs. In these cases, neutralizing activity against gp41 or quaternary epitopes may play a relatively small role in virus neutralization. However, a large fraction of the neutralizing activity in many plasmas could not be ascribed to Abs directed toward any of the known epitopes. This was particularly true for the subtype C plasmas. It is possible that antigenic differences in subtype B and C Envs translate into differences in the specificities of the broadly cross-reactive neutralizing activity that appears later in infection (43, 52). For example, subtype C plasmas may contain CD4bs NAb activity that is generally insensitive to the D368R mutation, unlike subtype B plasmas. We therefore tested a D368R E370A double mutant in native PAGE that might be expected to more completely knock out the CD4bs, but this did not reveal any additional CD4bs activity beyond that revealed by the D368R single mutant (not shown). We are now evaluating the effects of subtype-specific D368R mutations in subtype C Envs in gp120 adsorptions and trimer binding assays.

We considered activity directed to the C3/V4 domain as one possible explanation for the uncharacterized subtype C activity. The C3/V4 domain of subtype C Envs has been implicated in autologous neutralization of subtype C viruses following seroconversion (43, 52), but given the variability of this region in subtype C Envs, it was not clear if these NAbs might become cross-reactive during chronic infection. The results of preliminary studies indicated that Env-matched C3 peptides (see Fig. S6 in the supplemental material) did not interfere with subtype C neutralization in any case (data not shown), suggesting that C3 epitopes are not sufficiently conserved to be targets of broad neutralization activity. However, because we lack effective control NAbs directed to the C3 region, we have no way to ensure that our peptides can effectively adsorb C3 NAb activity per se.

The general conformity of the data from two assays designed to detect CD4bs NAbs reinforces and extends the findings of previous studies showing that CD4bs Abs are the only specificity defined to date that constitutes a significant portion of plasma NAb activity in broadly neutralizing plasmas (18, 35). The contributions of CD4bs Abs to the neutralization of different viruses also varied considerably. This is exemplified by the behavior of plasma 1686 (Fig. 3), in which CD4bs activity is responsible for the neutralization of tier 2 but not subtype B tier 1 isolates, where the effect of V3 Abs probably eclipses the effect of CD4bs NAbs. Therefore, the evaluation of any NAb specificity's contribution to neutralization should be carefully considered in context with other Abs that may also neutralize a given virus isolate.

We observed several cases in which plasmas were unusually potent against a particular tier 2 virus (Fig. 1). This may stem from the acute sensitivity of certain viruses to the predominant cross-neutralizing activity, which in some cases may be mediated by CD4bs NAbs (e.g., the potent neutralization of JR-FL by plasma 1686). However, there are other cases where the plasma neutralization specificity remains largely unidentified. For example, plasma BB75 neutralized viruses Du123 and ZA12 with ID_{50}s of 9,320 and 1,081, respectively, much higher than its titers of ~1:100 against most other viruses (Fig. 1). It seems likely that this arises from virus sensitivity to a particular specificity, which in these cases remains unknown.

Of the remaining known neutralizing specificities that might explain broad plasma neutralization, little evidence was found for 2G12-like NAbs. This is perhaps not entirely surprising, given that 2G12 exhibits a highly unusual domain swap configuration and targets a carbohydrate epitope that would be expected to be regulated by tolerance. Likewise, very little Ab against the gp41 MPER was detected in most cases. This latter finding may be consistent with the hypothesis that certain MPER Abs are regulated by tolerance due to their potential autoreactive capacity (25).

Plasma BB34 was exceptional in that it exhibited an extremely high titer of MPER-specific NAbs. The observed titer of 1:200 would require an estimated 67 μg/ml of 2F5, 600 μg/ml of 4E10, or 960 μg/ml of Z13e1. If the MPER NAb(s) in BB34 is similar to the latter two prototypes, then they would likely constitute an overwhelmingly dominant fraction of the overall anti-Env Ab response, considering previous estimates of 370 to 1,600 μg/ml of gp120 Ab in chronic HIV+ plasmas (4). In practice, it is unlikely that NAbs exactly similar to 2F5 or Z13e1 are responsible here, since the precise epitopes for these NAbs are absent in most subtype C Envs. This is consistent with results of a study of plasmas from patients infected with various subtypes against the MPER graft mutants that revealed common specificities that were somewhat distinct from the three well-known prototypes (2). Fine mapping of the BB34 plasma using the various MPER mutants will appear elsewhere (Gray and Morris, unpublished).

The results of simple calculations suggest that V3 Abs are likely to play little or no role in JR-FL neutralization in our analysis. Taking MAb 447-52D as an example, with a neutralization IC_{50} against JR-FL of ~30 μg/ml, the concentration that would be required to mediate a neutralization titer of 1:30 is 900 μg/ml, which is near the upper limit of total estimated anti-gp120 binding Abs found in patients with typical chronic infections. In contrast, for the primary subtype C isolate TV1, V3 loop adsorptions were effective regardless of the presence of any CD4bs NAbs (Fig. 8). This indicates that the TV1 virus,

in contrast to JR-FL, is largely insensitive to CD4bs NAbs in patient plasmas but is sensitive to V3 NAbs (Fig. 1). The subtype-specific differences in V3-mediated neutralization observed in the peptide interference studies were somewhat unexpected (Fig. 8). Though the V3 N terminus is well known to play a dominant role in the neutralization of subtype B tier 1 viruses (17, 36), the broad susceptibility of subtype C viruses to specificities targeting either V3 terminus is less well appreciated. Further studies with additional subtype C isolates will be required to confirm whether this observation indicates a subtype-specific difference in V3 loop orientation. However, the results of a recent study of polyvalent vaccine sera showed that subtype B immunogens elicit V3 loop Abs focused on the N terminus, while subtype C immunogens elicit V3 Abs that are more focused on the V3 crown (64). Other studies have also indicated that V3 Abs generated against other subtypes, including subtype C, can be more cross-subtype reactive (30, 31, 66). Overall, our data imply that only the N-terminal portion of the V3 loop of JR-FL.d301 is exposed, while both the N and C termini of the TV1 V3 loop are accessible.

In summary, we found that NAbs directed against the YU2 gp120 accounted for a substantial, although variable, fraction of the NAbs in many plasmas. A significant fraction of subtype B and a smaller fraction of subtype C plasma neutralization was directed against the CD4bs. This subtype difference could stem simply from the use of subtype B reagents in most of our assays, thereby preventing the identification of subtype C-specific epitope targets. Our prime intent here was to gain an appreciation of breadth both within and outside subtypes. We are now adapting our assays to subtype C to identify intrasubtype activity. MPER NAbs were generally rare, with one notable exception. As a result, our main finding was that the majority of neutralizing activity against JR-FL, particularly of subtype C plasmas, was unlike any of the few known broadly neutralizing MAbs that our mapping assays were designed to detect. Clearly, it would be of great interest to identify this activity, to provide an impetus for new vaccine designs. Accordingly, we are now developing panels of Env mutants, Env fragments, and modified assays to dissect these unknown specificities, which appear to be largely directed to gp120 (Fig. 3). These efforts may also assist in identifying Env constructs and methods that are well suited for selecting new NAbs from infected donors. In the future, we anticipate that a comprehensive mapping algorithm may assist the analysis of vaccine sera, such that informed adjustments can then be made to the vaccine to help refocus or amplify effective NAb responses.

ACKNOWLEDGMENTS

This study was supported by Bill and Melinda Gates Collaboration for AIDS Vaccine Discovery Vaccine Immune Monitoring Consortium grant number 38619. Additional support was provided by NIH RO1 AI58763 (J.M.B.), California HIV/AIDS Research Program grant ID06-TPI-211 at the University of California (J.M.B.), the AIDS and Infectious Disease Science Center at the Torrey Pines Institute for Molecular Studies (J.M.B.), Grand Challenges Grant number 37874 (G.M.S.), the South African AIDS Vaccine Initiative (SAAVI), and the intramural research program of the Vaccine Research Center, NIAID (E.A.L., D.W. and J.R.M.).

We thank T. Wrin for providing assistance in selecting subtype B plasmas; D. Burton for providing MAbs b12 and X5; H. Katinger for providing MAbs 2G12, 2F5, and 4E10; Susan Zolla-Pazner for providing MAb 447-52D; B. F. Haynes and H. X. Liao for providing consensus gp140 proteins; M. Zwick for providing MAb Z13e1; L. Stamatatos, B. Hahn, R. Desrosiers, and the NIH AIDS Repository for providing virus stocks and Env plasmids; and G. Nabel for the guinea pig serum. We thank Judy T. Lucas and Vicki C. Ashley for expert technical assistance and Brenda Hartman for assistance with graphics.

REFERENCES

1. **Abrahamyan, L. G., R. M. Markosyan, J. P. Moore, F. S. Cohen, and G. B. Melikyan.** 2003. Human immunodeficiency virus type 1 Env with an intersubunit disulfide bond engages coreceptors but requires bond reduction after engagement to induce fusion. J. Virol. **77:**5829–5836.
2. **Bibollet-Ruche, F., L. Hui, J. M. Decker, P. A. Geopfert, B. H. Hahn, E. Delaporte, M. Peeters, S. Allen, E. Hunter, J. Robinson, P. D. Kwong, and G. M. Shaw.** 2006. Detection of novel neutralizing antibody responses to the membrane proximal external region (MPER) or gp41 following infection by HIV-1 subtypes A, B, C, D, F, G, H, CRF01, CRF02, or CRF11, abstr. 110, p. 196. Keystone Symposium X6, HIV Vaccines, Keystone, CO, 27 March to 2 April.
3. **Binley, J. M., C. S. Cayanan, C. Wiley, N. Schulke, W. C. Olson, and D. R. Burton.** 2003. Redox-triggered infection by disulfide-shackled human immunodeficiency virus type 1 pseudovirions. J. Virol. **77:**5678–5684.
4. **Binley, J. M., P. J. Klasse, Y. Cao, I. Jones, M. Markowitz, D. D. Ho, and J. P. Moore.** 1997. Differential regulation of the antibody responses to Gag and Env proteins of human immunodeficiency virus type 1. J. Virol. **71:**2799–2809.
5. **Binley, J. M., T. Wrin, B. Korber, M. B. Zwick, M. Wang, C. Chappey, G. Stiegler, R. Kunert, S. Zolla-Pazner, H. Katinger, C. J. Petropoulos, and D. R. Burton.** 2004. Comprehensive cross-clade neutralization analysis of a panel of anti-human immunodeficiency virus type 1 monoclonal antibodies. J. Virol. **78:**13232–13252.
6. **Bou-Habib, D. C., G. Roderiquez, T. Oravecz, P. W. Berman, P. Lusso, and M. A. Norcross.** 1994. Cryptic nature of envelope V3 region epitopes protects primary monocytotropic human immunodeficiency virus type 1 from antibody neutralization. J. Virol. **68:**6006–6013.
7. **Braibant, M., S. Brunet, D. Costagliola, C. Rouzioux, H. Agut, H. Katinger, B. Autran, and F. Barin.** 2006. Antibodies to conserved epitopes of the HIV-1 envelope in sera from long-term non-progressors: prevalence and association with neutralizing activity. AIDS **20:**1923–1930.
8. **Brown, B. K., L. Wieczorek, E. Sanders-Buell, A. R. Borges, M. L. Robb, D. L. Birx, N. L. Michael, F. E. McCutchan, and V. R. Polonis.** 2008. Cross-clade neutralization patterns among HIV-1 strains from the six major clades of the pandemic evaluated and compared in two different models. Virology **375:**529–538.
9. **Bunnik, E. M., L. Pisas, A. C. van Nuenen, and H. Schuitemaker.** 2008. Autologous neutralizing humoral immunity and evolution of the viral envelope in the course of subtype B human immunodeficiency virus type 1 infection. J. Virol. **82:**7932–7941.
10. **Burton, D. R., J. Pyati, R. Koduri, S. J. Sharp, G. B. Thornton, P. W. Parren, L. S. Sawyer, R. M. Hendry, N. Dunlop, P. L. Nara, et al.** 1994. Efficient neutralization of primary isolates of HIV-1 by a recombinant human monoclonal antibody. Science **266:**1024–1027.
11. **Cheng-Mayer, C., R. Liu, N. R. Landau, and L. Stamatatos.** 1997. Macrophage tropism of human immunodeficiency virus type 1 and utilization of the CC-CKR5 coreceptor. J. Virol. **71:**1657–1661.
12. **Crooks, E. T., P. Jiang, M. Franti, S. Wong, M. B. Zwick, J. A. Hoxie, J. E. Robinson, P. L. Moore, and J. M. Binley.** 2008. Relationship of HIV-1 and SIV envelope glycoprotein trimer occupation and neutralization. Virology **377:**364–378.
13. **Crooks, E. T., P. L. Moore, M. Franti, C. S. Cayanan, P. Zhu, P. Jiang, R. P. de Vries, C. Wiley, I. Zharkikh, N. Schülke, K. H. Roux, D. C. Montefiori, D. R. Burton, and J. M. Binley.** 2007. A comparative immunogenicity study of HIV-1 virus-like particles bearing various forms of envelope proteins, particles bearing no envelope and soluble monomeric gp120. Virology **366:**245–262.
14. **Crooks, E. T., P. L. Moore, D. Richman, J. Robinson, J. A. Crooks, M. Franti, N. Schulke, and J. M. Binley.** 2005. Characterizing anti-HIV monoclonal antibodies and immune sera by defining the mechanism of neutralization. Hum. Antibodies **14:**101–113.
15. **D'Amelio, R., R. Biselli, R. Nisini, P. M. Matricardi, A. Aiuti, I. Mezzaroma, E. Pinter, O. Pontesilli, and F. Aiuti.** 1992. Spectrotype of anti-gp120 antibodies remains stable during the course of HIV disease. J. Acquir. Immune Defic. Syndr. **5:**930–935.
16. **Decker, J. M., F. Bibollet-Ruche, X. Wei, S. Wang, D. N. Levy, W. Wang, E. Delaporte, M. Peeters, C. A. Derdeyn, S. Allen, E. Hunter, M. S. Saag, J. A. Hoxie, B. H. Hahn, P. D. Kwong, J. E. Robinson, and G. M. Shaw.** 2005. Antigenic conservation and immunogenicity of the HIV coreceptor binding site. J. Exp. Med. **201:**1407–1419.
17. **Derby, N. R., Z. Kraft, E. Kan, E. T. Crooks, S. W. Barnett, I. K. Srivastava, J. M. Binley, and L. Stamatatos.** 2006. Antibody responses elicited in macaques immunized with human immunodeficiency virus type 1 (HIV-1) SF162-derived gp140 envelope immunogens: comparison with those elicited

during homologous simian/human immunodeficiency virus SHIVSF162P4 and heterologous HIV-1 infection J. Virol. **80:**8745–8762.

18. **Dhillon, A. K., H. Donners, R. Pantophlet, W. E. Johnson, J. M. Decker, G. M. Shaw, F.-H. Lee, D. D. Richman, R. W. Doms, G. Vanham, and D. R. Burton.** 2007. Dissecting the neutralizing antibody specificities of broadly neutralizing sera from human immunodeficiency virus type 1-infected donors. J. Virol. **81:**6548–6562.
19. **Fouts, T. R., J. M. Binley, A. Trkola, J. E. Robinson, and J. P. Moore.** 1997. Neutralization of the human immunodeficiency virus type 1 primary isolate JR-FL by human monoclonal antibodies correlates with antibody binding to the oligomeric form of the envelope glycoprotein complex. J. Virol. **71:**2779–2785.
20. **Gao, F., S. G. Morrison, D. L. Robertson, C. L. Thornton, S. Craig, G. Karlsson, J. Sodroski, M. Morgado, B. Galvao-Castro, and H. von Briesen, S. Beddows, J. Weber, P. M. Sharp, G. M. Shaw, B. H. Hahn, and the WHO and NIAID Networks for HIV Isolation and Characterization.** 1996. Molecular cloning and analysis of functional envelope genes from human immunodeficiency virus type 1 sequence subtypes A through G. J. Virol. **70:**1651–1667.
21. **Gao, F., E. A. Weaver, Z. Lu, Y. Li, H.-X. Liao, B. Ma, S. M. Alam, R. M. Scearce, L. L. Sutherland, J.-S. Yu, J. M. Decker, G. M. Shaw, D. C. Montefiori, B. T. Korber, B. H. Hahn, and B. F. Haynes.** 2005. Antigenicity and immunogenicity of a synthetic human immunodeficiency virus type 1 group M consensus envelope glycoprotein. J. Virol. **79:**1154–1163.
22. **Gorny, M. K., L. Stamatatos, B. Volsky, K. Revesz, C. Williams, X. H. Wang, S. Cohen, R. Staudinger, and S. Zolla-Pazner.** 2005. Identification of a new quaternary neutralizing epitope on human immunodeficiency virus type 1 virus particles. J. Virol. **79:**5232–5237.
23. **Gray, E. S., P. L. Moore, F. Bibollet-Ruche, H. Li, J. M. Decker, T. Meyers, G. M. Shaw, and L. Morris.** 2008. 4E10-resistant variants in a human immunodeficiency virus type 1 subtype C-infected individual with an anti-membrane-proximal external region-neutralizing antibody response. J. Virol. **82:**2367–2375.
24. **Harouse, J. M., A. Gettie, T. Eshetu, R. C. Tan, R. Bohm, J. Blanchard, G. Baskin, and C. Cheng-Mayer.** 2001. Mucosal transmission and induction of simian AIDS by CCR5-specific simian/human immunodeficiency virus SHIV(SF162P3). J. Virol. **75:**1990–1995.
25. **Haynes, B. F., J. Fleming, E. W. St. Clair, H. Katinger, G. Stiegler, R. Kunert, J. Robinson, R. M. Scearce, K. Plonk, H. F. Staats, T. L. Ortel, H. X. Liao, and S. M. Alam.** 2005. Cardiolipin polyspecific autoreactivity in two broadly neutralizing HIV-1 antibodies. Science **308:**1906–1908.
26. **Haynes, B. F., and D. C. Montefiori.** 2006. Aiming to induce broadly reactive neutralizing antibody responses with HIV-1 vaccine candidates. Expert Rev. Vaccines **5:**347–363.
27. **He, Y., W. J. Honnen, C. P. Krachmarov, M. Burkhart, S. C. Kayman, J. Corvalan, and A. Pinter.** 2002. Efficient isolation of novel human monoclonal antibodies with neutralizing activity against HIV-1 from transgenic mice expressing human Ig loci. J. Immunol. **169:**595–605.
28. **Keele, B. F., E. E. Giorgi, J. F. Salazar-Gonzalez, J. M. Decker, K. T. Pham, M. G. Salazar, C. Sun, T. Grayson, S. Wang, H. Li, X. Wei, C. Jiang, J. L. Kirchherr, F. Gao, J. A. Anderson, L. H. Ping, R. Swanstrom, G. D. Tomaras, W. A. Blattner, P. A. Goepfert, J. M. Kilby, M. S. Saag, E. L. Delwart, M. P. Busch, M. S. Cohen, D. C. Montefiori, B. F. Haynes, B. Gaschen, G. S. Athreya, H. Y. Lee, N. Wood, C. Seoighe, A. S. Perelson, T. Bhattacharya, B. T. Korber, B. H. Hahn, and G. M. Shaw.** 2008. Identification and characterization of transmitted and early founder virus envelopes in primary HIV-1 infection. Proc. Natl. Acad. Sci. USA **105:**7552–7557.
29. **Kolchinsky, P., E. Kiprilov, and J. Sodroski.** 2001. Increased neutralization sensitivity of CD4-independent human immunodeficiency virus variants. J. Virol. **75:**2041–2050.
30. **Krachmarov, C., A. Pinter, W. J. Honnen, M. K. Gorny, P. N. Nyambi, S. Zolla-Pazner, and S. C. Kayman.** 2005. Antibodies that are cross-reactive for human immunodeficiency virus type 1 clade A and clade B V3 domains are common in patient sera from Cameroon, but their neutralization activity is usually restricted by epitope masking. J. Virol. **79:**780–790.
31. **Krachmarov, C. P., W. J. Honnen, S. C. Kayman, M. K. Gorny, S. Zolla-Pazner, and A. Pinter.** 2006. Factors determining the breadth and potency of neutralization by V3-specific human monoclonal antibodies derived from subjects infected with clade A or clade B strains of human immunodeficiency virus type 1. J. Virol. **80:**7127–7135.
32. **Kraft, Z., N. R. Derby, R. A. McCaffrey, R. Niec, W. M. Blay, N. L. Haigwood, E. Moysi, C. J. Saunders, T. Wrin, C. J. Petropoulos, M. J. McElrath, and L. Stamatatos.** 2007. Macaques infected with a CCR5-tropic simian/human immunodeficiency virus (SHIV) develop broadly reactive anti-HIV neutralizing antibodies. J. Virol. **81:**6402–6411.
33. **Li, M., F. Gao, J. R. Mascola, L. Stamatatos, V. R. Polonis, M. Koutsoukos, G. Voss, P. Goepfert, P. Gilbert, K. M. Greene, M. Bilska, D. L. Kothe, J. F. Salazar-Gonzalez, X. Wei, J. M. Decker, B. H. Hahn, and D. C. Montefiori.** 2005. Human immunodeficiency virus type 1 *env* clones from acute and early subtype B infections for standardized assessments of vaccine-elicited neutralizing antibodies. J. Virol. **79:**10108–10125.
34. **Li, M., J. F. Salazar-Gonzalez, C. A. Derdeyn, L. Morris, C. Williamson, J. E. Robinson, J. M. Decker, Y. Li, M. G. Salazar, V. R. Polonis, K. Mlisana, S. A. Karim, K. Hong, K. M. Greene, M. Bilska, J. Zhou, S. Allen, E. Chomba, J. Mulenga, C. Vwalika, F. Gao, M. Zhang, B. T. Korber, E. Hunter, B. H. Hahn, and D. C. Montefiori.** 2006. Genetic and neutralization properties of subtype C human immunodeficiency virus type 1 molecular *env* clones from acute and early heterosexually acquired infections in Southern Africa. J. Virol. **80:**11776–11790.
35. **Li, Y., S. Migueles, B. Welcher, K. Svehla, A. Phogat, M. K. Louder, X. Wu, G. M. Shaw, M. Connors, R. T. Wyatt, and J. M. Mascola.** 2007. Broad HIV-1 neutralization mediated by CD4 binding site antibodies. Nat. Med. **13:**1032–1034.
36. **Li, Y., K. Svehla, N. L. Mathy, G. Voss, J. R. Mascola, and R. Wyatt.** 2006. Characterization of antibody responses elicited by human immunodeficiency virus type 1 primary isolate trimeric and monomeric envelope glycoproteins in selected adjuvants. J. Virol. **80:**1414–1426.
37. **Liao, H. X., L. L. Sutherland, S. M. Xia, M. E. Brock, R. M. Scearce, S. Vanleeuwen, S. M. Alam, M. McAdams, E. A. Weaver, Z. Camacho, B. J. Ma, Y. Li, J. M. Decker, G. J. Nabel, D. C. Montefiori, B. H. Hahn, B. T. Korber, F. Gao, and B. F. Haynes.** 2006. A group M consensus envelope glycoprotein induces antibodies that neutralize subsets of subtype B and C HIV-1 primary viruses. Virology **353:**268–282.
38. **Mascola, J. R., P. D'Souza, P. Gilbert, B. H. Hahn, N. L. Haigwood, L. Morris, C. J. Petropoulos, V. R. Polonis, M. Sarzotti, and D. C. Montefiori.** 2005. Recommendations for the design and use of standard virus panels to assess neutralizing antibody responses elicited by candidate human immunodeficiency virus type 1 vaccines. J. Virol. **79:**10103–10107.
39. **Migueles, S. A., A. C. Laborico, W. L. Shupert, M. S. Sabbaghian, R. Rabin, C. W. Hallahan, D. Van Baarle, S. Kostense, F. Miedema, M. McLaughlin, L. Ehler, J. Metcalf, S. Liu, and M. Connors.** 2002. HIV-specific CD8+ T cell proliferation is coupled to perforin expression and is maintained in nonprogressors. Nat. Immunol. **3:**1061–1068.
40. **Moore, J. P., Y. Cao, D. D. Ho, and R. A. Koup.** 1994. Development of the anti-gp120 antibody response during seroconversion to human immunodeficiency virus type 1. J. Virol. **68:**5142–5155.
41. **Moore, J. P., and J. Sodroski.** 1996. Antibody cross-competition analysis of the human immunodeficiency virus type 1 gp120 exterior envelope glycoprotein. J. Virol. **70:**1863–1872.
42. **Moore, P. L., E. T. Crooks, L. Porter, P. Zhu, C. S. Cayanan, H. Grise, P. Corcoran, M. B. Zwick, M. Franti, L. Morris, K. H. Roux, D. R. Burton, and J. M. Binley.** 2006. Nature of nonfunctional envelope proteins on the surface of human immunodeficiency virus type 1. J. Virol. **80:**2515–2528.
43. **Moore, P. L., E. S. Gray, I. A. Choge, N. Ranchobe, K. Mlisana, S. S. A. Karim, C. Williamson, L. Morris, and the CAPRISA 002 Study Team.** 2008. The C3-V4 region is a major target of autologous neutralizing antibodies in human immunodeficiency virus-1 subtype C infection. J. Virol. **82:**1860–1869.
44. **Nelson, J. D., F. M. Brunel, R. Jensen, E. T. Crooks, R. M. Cardoso, M. Wang, A. Hessell, I. A. Wilson, J. M. Binley, P. E. Dawson, D. R. Burton, and M. B. Zwick.** 2007. An affinity-enhanced neutralizing antibody against the membrane-proximal external region of human immunodeficiency virus type 1 gp41 recognizes an epitope between those of 2F5 and 4E10. J. Virol. **81:**4033–4043.
45. **Pantophlet, R., R. O. Aguilar-Sino, T. Wrin, L. A. Cavacini, and D. R. Burton.** 2007. Analysis of the neutralization breadth of the anti-V3 antibody F425-B4e8 and re-assessment of its epitope fine specificity by scanning mutagenesis. Virology **364:**441–453.
46. **Pantophlet, R., and D. R. Burton.** 2006. GP120: target for neutralizing HIV-1 antibodies. Annu. Rev. Immunol. **24:**739–769.
47. **Phogat, S., K. Svehla, M. Tang, A. Spadaccini, J. Muller, J. Mascola, I. Berkower, and R. Wyatt.** 2008. Analysis of the human immunodeficiency virus type 1 gp41 membrane proximal external region arrayed on hepatitis B surface antigen particles. Virology **373:**72–84.
48. **Phogat, S., R. T. Wyatt, and G. B. Karlsson Hedestam.** 2007. Inhibition of HIV-1 entry by antibodies: potential viral and cellular targets. J. Intern. Med. **262:**26–43.
49. **Quakkelaar, E. D., F. P. van Alphen, B. D. Boeser-Nunnink, A. C. van Nuenen, R. Pantophlet, and H. Schuitemaker.** 2007. Susceptibility of recently transmitted subtype B human immunodeficiency virus type 1 variants to broadly neutralizing antibodies. J. Virol. **81:**8533–8542.
50. **Richman, D. D., T. Wrin, S. J. Little, and C. J. Petropoulos.** 2003. Rapid evolution of the neutralizing antibody response to HIV type 1 infection. Proc. Natl. Acad. Sci. USA **100:**4144–4149.
51. **Roben, P., J. P. Moore, M. Thali, J. Sodroski, C. F. Barbas III, and D. R. Burton.** 1994. Recognition properties of a panel of human recombinant Fab fragments to the CD4 binding site of gp120 that show differing abilities to neutralize human immunodeficiency virus type 1. J. Virol. **68:**4821–4828.
52. **Rong, R., S. Gnanakaran, J. M. Decker, F. Bibollet-Ruche, J. Taylor, J. N. Sfakianos, J. L. Mokili, M. Muldoon, J. Mulenga, S. Allen, B. H. Hahn, G. M. Shaw, J. L. Blackwell, B. T. Korber, E. Hunter, and C. A. Derdeyn.** 2007. Unique mutational patterns in the envelope alpha 2 amphipathic helix and acquisition of length in gp120 hypervariable domains are associated with

resistance to autologous neutralization of subtype C human immunodeficiency virus type 1. J. Virol. **81:**5658–5668.

53. **Salazar-Gonzalez, J. F., E. Bailes, K. T. Pham, M. G. Salazar, M. B. Guffey, B. F. Keele, C. A. Derdeyn, P. Farmer, E. Hunter, S. Allen, O. Manigart, J. Mulenga, J. A. Anderson, R. Swanstrom, B. F. Haynes, G. S. Athreya, B. T. Korber, P. M. Sharp, G. M. Shaw, and B. H. Hahn.** 2008. Deciphering human immunodeficiency virus type 1 transmission and early envelope diversification by single-genome amplification and sequencing. J. Virol. **82:** 3952–3970.
54. **Sanchez-Martinez, S., M. Lorizate, H. Katinger, R. Kunert, and J. L. Nieva.** 2006. Membrane association and epitope recognition by HIV-1 neutralizing anti-gp41 2F5 and 4E10 antibodies. AIDS Res. Hum. Retroviruses **22:**998–1006.
55. **Sanders, R. W., M. Venturi, L. Schiffner, R. Kalyanaraman, H. Katinger, K. O. Lloyd, P. D. Kwong, and J. P. Moore.** 2002. The mannose-dependent epitope for neutralizing antibody 2G12 on human immunodeficiency virus type 1 glycoprotein gp120. J. Virol. **76:**7293–7305.
56. **Sattentau, Q. J., and J. P. Moore.** 1995. Human immunodeficiency virus type 1 neutralization is determined by epitope exposure on the gp120 oligomer. J. Exp. Med. **182:**185–196.
57. **Scanlan, C. N., R. Pantophlet, M. R. Wormald, E. Ollmann Saphire, R. Stanfield, I. A. Wilson, H. Katinger, R. A. Dwek, P. M. Rudd, and D. R. Burton.** 2002. The broadly neutralizing anti-human immunodeficiency virus type 1 antibody 2G12 recognizes a cluster of $\alpha 1 \rightarrow 2$ mannose residues on the outer face of gp120. J. Virol. **76:**7306–7321.
58. **Schulke, N., M. S. Vesanen, R. W. Sanders, P. Zhu, M. Lu, D. J. Anselma, A. R. Villa, P. W. Parren, J. M. Binley, K. H. Roux, P. J. Maddon, J. P. Moore, and W. C. Olson.** 2002. Oligomeric and conformational properties of a proteolytically mature, disulfide-stabilized human immunodeficiency virus type 1 gp140 envelope glycoprotein. J. Virol. **76:**7760–7776.
59. **Seaman, M. S., D. F. Leblanc, L. E. Grandpre, M. T. Bartman, D. C. Montefiori, N. L. Letvin, and J. R. Mascola.** 2007. Standardized assessment of NAb responses elicited in rhesus monkeys immunized with single- or multi-clade HIV-1 envelope immunogens. Virology **367:**175–186.
60. **Sharon, M., N. Kessler, R. Levy, S. Zolla-Pazner, M. Gorlach, and J. Anglister.** 2003. Alternative conformations of HIV-1 V3 loops mimic beta hairpins in chemokines, suggesting a mechanism for coreceptor selectivity. Structure **11:**225–236.
61. **Stamatatos, L., M. Wiskerchen, and C. Cheng-Mayer.** 1998. Effect of major deletions in the V1 and V2 loops of a macrophage-tropic HIV type 1 isolate on viral envelope structure, cell entry, and replication. AIDS Res. Hum. Retrovir. **14:**1129–1139.
62. **Suarez, T., S. Nir, F. M. Goni, A. Saez-Cirion, and J. L. Nieva.** 2000. The pre-transmembrane region of the human immunodeficiency virus type-1 glycoprotein: a novel fusogenic sequence. FEBS Lett. **477:**145–149.
63. **Trkola, A., H. Kuster, P. Rusert, B. Joos, M. Fischer, C. Leemann, A. Manrique, M. Huber, M. Rehr, A. Oxenius, R. Weber, G. Stiegler, B. Vcelar, H. Katinger, L. Aceto, and H. F. Gunthard.** 2005. Delay of HIV-1 rebound after cessation of antiretroviral therapy through passive transfer of human neutralizing antibodies. Nat. Med. **11:**615–622.
64. **Vaine, M., S. Wang, E. T. Crooks, P. Jiang, D. C. Montefiori, J. Binley, and S. Lu.** 2008. Improved induction of antibodies against key neutralizing epitopes by human immunodeficiency virus type 1 gp120 DNA prime-protein boost vaccination compared to gp120 protein only vaccination. J. Virol. **82:**7369–7378.
65. **Wei, X., J. M. Decker, S. Wang, H. Hui, J. C. Kappes, X. Wu, J. F. Salazar-Gonzalez, M. G. Salazar, J. M. Kilby, M. S. Saag, N. L. Komarova, M. A. Nowak, B. H. Hahn, P. D. Kwong, and G. M. Shaw.** 2003. Antibody neutralization and escape by HIV-1. Nature **422:**307–312.
66. **Wu, L., Z. Y. Yang, L. Xu, B. Welcher, S. Winfrey, Y. Shao, J. R. Mascola, and G. J. Nabel.** 2006. Cross-clade recognition and neutralization by the V3 region from clade C human immunodeficiency virus-1 envelope. Vaccine **24:**4995–5002.
67. **Xiang, S.-H., N. Doka, R. K. Choudhary, J. Sodroski, and J. E. Robinson.** 2002. Characterization of CD4-induced epitopes on the HIV-1 gp120 envelope glycoprotein recognized by neutralizing human monoclonal antibodies. AIDS Res. Hum. Retrovir. **18:**1207–1217.
68. **Yang, X., V. Tomov, S. Kurteva, L. Wang, X. Ren, M. K. Gorny, S. Zolla-Pazner, and J. Sodroski.** 2004. Characterization of the outer domain of the gp120 glycoprotein from human immunodeficiency virus type 1. J. Virol. **78:**12975–12986.
69. **Yuste, E., H. B. Sanford, J. Carmody, J. Bixby, S. Little, M. B. Zwick, T. Greenough, D. R. Burton, D. D. Richman, R. C. Desrosiers, and W. E. Johnson.** 2006. Simian immunodeficiency virus engrafted with human immunodeficiency virus type 1 (HIV-1)-specific epitopes: replication, neutralization, and survey of HIV-1-positive plasma. J. Virol. **80:**3030–3041.
70. **Zolla-Pazner, S., S. S. Cohen, C. Krachmarov, S. Wang, A. Pinter, and S. Lu.** 2008. Focusing the immune response on the V3 loop, a neutralizing epitope of the HIV-1 gp120 envelope. Virology **372:**233–246.
71. **Zwick, M. B., E. O. Saphire, and D. R. Burton.** 2004. gp41: HIV's shy protein. Nat. Med. **10:**133–134.